Physics – Uspekhi **42** (3) 215 – 243 (1999)

REVIEWS OF TOPICAL PROBLEMS PACS numbers: **71.27. + a, 74.90. + n**, 74.25.Jb

Spin-fluctuation mechanism of high-T_c superconductivity and order-parameter symmetry

Yu A Izyumov

Contents

Abstract. The notion that electrons in high-T_c cuprates pair via antiferromagnetic spin fluctuations is discussed and the symmetry of the superconducting order parameter is analyzed. Three approaches to the problem, one phenomenological (with an experimental dynamic magnetic susceptibility) and two microscopic (involving, respectively, the Hubbard model and the *tJ*-model) are considered and it is shown that in each case strong-coupling theory leads to a d-wave order parameter with zeros at the Fermi surface. The review then proceeds to consider experimental techniques in which the d-symmetry of the order parameter may manifest itself. These include low-temperature thermodynamic measurements, measurements of the penetration depth and the upper critical field, Josephson junction experiments to obtain the phase of the superconducting order parameter, and various spectroscopic methods. The experimental data suggest that the order parameter in cuprates is $d_{x^2-y^2}$-wave. Ginzburg – Landau theory for a superconductor with a d-wave order parameter is outlined and both an isolated vortex and a vortex lattice are investigated. Finally, some theoretical aspects of the effects of nonmagnetic impurities on a d-wave superconductor are considered.

1. Introduction

Over the years a vast body of experimental data has been collected that suggests that an anisotropic superconducting order parameter is realized in high-T_c superconductors of the metal-oxide group. Moreover, there are strong indications (provided by experiments) that the order parameter is d-symmetric. A natural explanation of this symmetry stems from the concept of the spin-fluctuation mechanism of electron pairing.[1] Thus, both phenomena, electron pairing due to exchange of spin excitations and the d-wave nature of a Cooper pair, are closely related, and experimental verification of one of these phenomena suggests, at least indirectly, that the second also exists.

The hypothesis of the spin-fluctuation pairing mechanism is corroborated by the fact that, being the parents of the lanthanum [denoted (214)] and yttrium [denoted (123)] systems, the stoichiometric compounds La_2CuO_4 and

Yu A Izyumov Institute of Metal Physics, Ural Division of the Russian Academy of Sciences, ul. S Kovalevskoĭ 18, 620219 Ekaterinburg, Russia
Tel. (7-3432) 74 41 93
Fax (7-3432) 74 52 44
E-mail: izyumov@ifm.e-burg.su

Received 13 March 1998, revised 10 September 1998
Uspekhi Fizicheskikh Nauk **169** (3) 225 – 254 (1999)
Translated by E M Yankovsky; edited by A I Yaremchuk

[1] Akhiezer and Pomeranchuk [78] were the first to put forward the idea of electron pairing via spin fluctuations. They found that the indirect interaction of electrons via spin waves in a ferromagnetic metal manifests itself as an attraction to a triplet state and, hence, may lead to triplet pairing.

$YBa_2Cu_3O_6$ are antiferromagnetic insulators. Doping a (214) compound with strontium or a (123) compound with oxygen results in the emergence of a metallic state and superconductivity (e. g. see the latest reviews in Refs [1] and [2]). The fact that theses doped systems are close to an antiferromagnetic transition with the wave vector $\mathbf{Q} = (\pi, \pi)$ explains the importance of spin fluctuations in the interaction with which the quasiparticle spectrum of electrons is formed, and may simultaneously lead to Cooper pairing.

Many theoretical studies of high-T_c compounds that belong to the class of strongly correlated systems are made using the Hubbard model [3], which describes the hopping of electrons from site to site with a matrix element t for nearest neighbors and with Coulomb repulsion U when the electrons are at the same site. The model starts with the Hamiltonian

$$H = -t \sum_{ij\sigma} C_{i\sigma}^{\dagger} C_{j\sigma} + U \sum_{i} n_{i\uparrow} n_{i\downarrow} , \tag{1.1}$$

where $C_{i\sigma}(C_{i\sigma}^{\dagger})$ is the operator of annihilation (creation) of an electron at site i with spin σ, and $n_{i\sigma} = C_{i\sigma}^{\dagger} C_{i\sigma}$ is the number of electrons at the site. Magnetically ordered phases may form when the values of the parameters t and U and the electron concentration n lie within a certain range. Near the boundary of such a phase on the paramagnetic side there are strong fluctuations of the magnetic order parameter (or paramagnons). The nature of the indirect interaction of electrons via paramagnons near the region of the ferromagnetic instability region was studied many years ago by Berk and Schrieffer [4]. They found that the interaction is repulsive in the singlet channel, with the result that it inhibits ordinary superconductivity.

Later it was discovered that the situation near an antiferromagnetic instability is different. This becomes especially evident if one studies the behavior of spin susceptibility in the random-phase approximation (RPA). The susceptibility is determined by the bare electron spectrum (in what follows only a two-dimensional system corresponding to CuO planes in cuprates is examined)

$$\varepsilon(\mathbf{k}) = -2t(\cos k_x + \cos k_y) \tag{1.2}$$

and the chemical potential μ corresponding to the given electron concentration n. When the band is half-filled ($n = 1$), the spectrum has a nesting at the wave vector $\mathbf{q} = \mathbf{Q}$, which corresponds to a sharp peak in the spin susceptibility near this point. This means that the system is unstable with respect to the formation of an antiferromagnetic (Neel) state with a wave vector $\mathbf{Q}$ and that spin fluctuations are stronger near the point of magnetic phase transition. The contribution of the interaction with the fluctuations to the electron self-energy Σ is given by the following diagram:

$\Sigma(k) =$

, (1.3)

where the solid line and the dashed curve correspond, respectively, to the electron and spin-fluctuation (paramagnon) Green's functions, and the bare vertex corresponds to $\sim U$. Equation (1.3) for the superconducting phase is the Eliashberg equation [5] for the case of spin-fluctuation pairing. Scalapino et al. [6] and Bickers et al. [7] used this equation for systems with antiferromagnetic instability. For a half-filled band, when there is antiferromagnetic instability in the system, a numerical solution of the Eliashberg equation shows that the superconducting order parameter is $d_{x^2-y^2}$-wave, i.e. the gap depends on the wave vector as follows:

$$\Delta_d(\mathbf{k}) = \Delta_0(\cos k_x - \cos k_y) . \tag{1.4}$$

This was the first indication that in spin-fluctuation coupling the order parameter is d-wave. However, the values obtained for the superconducting transition temperature proved to be low: $T_c < 10^{-3}\, t$. Thus, although the theory of Scalapino et al. [6] did not explain high-T_c superconductivity, it revealed the connection between spin-fluctuation pairing and the d-wave nature of the superconducting order parameter. The modern bases of the spin-fluctuation mechanism of high-T_c superconductivity essentially stem from this approach (see also Refs [8] and [9]).

The gap specified by Eqn (1.4) is an alternating-sign function of the wave vector (Fig. 1); it vanishes on the diagonals of a square lattice (the first Brillouin zone). These 'zero lines' in the $\mathbf{k}$ space make $d_{x^2-y^2}$-paring more energy-suitable in the case of the spin-fluctuation mechanism. Indeed, the effective electron interaction via fluctuations of the antiferromagnetic order parameter is repulsive if the interacting electrons are at a single site (the initial Hamiltonian (1.1) takes this fact into account) and attractive if the interacting electrons are at different sites:

$$V_{\text{eff}}(\mathbf{R}) = V_0 \delta(\mathbf{R}) - V_1 \sum_{\mathbf{a}} \delta(\mathbf{R} - \mathbf{a}) , \tag{1.5}$$

where $\mathbf{R}$ is the radius vector for two electrons in the lattice, and $\mathbf{a}$ is the nearest-neighbor radius vector. This fact is discussed in Section 2, where we also see that the interaction of an electron at the center of the square lattice and an electron at any site on a diagonal of the square lattice is also repulsive. Figure 1a shows that the wave function of a Cooper pair vanishes precisely on the diagonals of the square, with the result that the repulsive interaction on these diagonals has no influence on the pair, and a $d_{x^2-y^2}$-wave Cooper pair survives even if U is large.

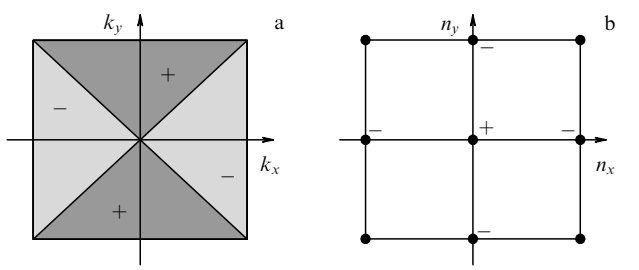

Figure 1. Sign distributions of (a) the gap function within the first Brillouin zone and (b) the effective electron–electron interaction with a unit cell for a square lattice in the case of the spin-fluctuation pairing mechanism.

A superconductor with d-pairing should have exotic properties that could be detected in experiments. Many of these features stem from the presence of zeros in the order parameter. Long before the discovery of high-T_c superconductivity, Volovik and Gor'kov [10] developed a phenomenological theory of superconductors with an anisotropic order parameter. The development of this theory was stimulated by the discovery of anomalies of superconductiv-

ity in heavy-fermion systems. A characteristic feature of such systems is superconductivity with an anisotropic order parameter, which vanishes at points on the Fermi surface. At low temperatures, the quasiparticle spectrum near these points must yield not an exponential contribution (as in ordinary isotropic superconductors) but a power-law contribution to thermodynamic properties: specific heat, NMR characteristics, and depth of magnetic-field penetration. The discovery of such power-law contributions would point to nontrivial behavior of the order parameter with zeros at the Fermi surface.

The arrangement of the order-parameter zeros is determined by the symmetry of the Cooper-pair wave function, which in turn is determined by the symmetry of the crystal. The realisable symmetries for a two-dimensional tetragonal crystal (a square lattice) were studied by Sigrist and Rice [11], who used group-representation theory. It is the basis functions of the corresponding irreducible representations that determine the possible dependence of the order parameter on the wave vector. For the $d_{x^2-y^2}$-wave case this dependence is given by Eqn (1.4). Along with d-symmetry we must consider s-symmetry, for which we can select two sets of basis functions,

$$\Delta_s(\mathbf{k}) = \Delta_0\,; \qquad \Delta_{s^*}(\mathbf{k}) = \Delta_0(\cos k_x + \cos k_y)\,, \tag{1.6}$$

which describe isotropic and anisotropic pairing. The s*-wave anisotropic order parameter also has zeros, which lie not on the diagonals $k_y = \pm k_x$ of the square but on the lines $k_y = \pi \pm k_x$. This means that a power-law temperature dependence observed in superconducting cuprates only suggests that the superconducting order parameter has zeros but does not make it possible to distinguish between $d_{x^2-y^2}$- and s*-symmetries — measuring other properties of the superconducting state could do this.

In recent years many experimental methods for determining the symmetry of the order parameter have been developed. Some of these methods (in which the Josephson current is measured in one way or another) deal with measurements of complex order parameter, while in others the gap in the quasiparticle spectrum is measured for different directions of the wave vector. The latter group includes spectroscopic experiments, which primarily use ARPES, infrared spectroscopy, and neutron spectroscopy. Experiments in which the effect of nonmagnetic impurities on the superconducting properties is studied form a special group. This effect strongly depends on what symmetry, s or d, the superconducting order parameter has. The experimental data for different high-T_c compounds irrevocably indicate that an anisotropic order parameter is realized and that the probability that this will be a $d_{x^2-y^2}$-wave order parameter is very high. The last argument is a serious argument in favor of the spin-fluctuation mechanism of high-T_c superconductivity.

In this review we elaborate on the concept of superconducting pairing through exchange of dynamic spin fluctuations and discuss all the results of studies dealing with the symmetry of the superconducting order parameter in high-T_c compounds of the copper-oxide group. In Sections 2–4 we discuss the existing theoretical approaches to the problem of spin-fluctuation interaction. One approach, which is being actively developed by Pines and collaborators [12], uses a phenomenological magnetic susceptibility with parameters taken from experiments on cuprates. The other two approaches are based on very simple models, which allow for the Coulomb interaction of electrons in the weak- and strong-coupling limits. The results of numerical calculations in all three approaches indicate that the order parameter is d-wave. In Sections 5–7 we discuss the properties of superconductors with a d-wave order parameter. We begin by using the Ginzburg–Landau theory to study the behavior of an isolated vortex in such superconductors and the properties of the vortex lattice. We then turn to the various experiments in which the symmetry of the order parameter manifests itself. We also investigate the result of studies of high-T_c cuprates. The review is concluded by a discussion of the role of impurities in superconductors with an anisotropic order parameter.

2. Superconductivity in a nearly antiferromagnetic Fermi liquid

2.1 The phenomenological approach in spin-fluctuation theory

The idea of a spin-fluctuation mechanism of high-T_c superconductivity that uses a phenomenological approach and the experimental data was proposed [13–17] long before the full development of the microscopic description of high-T_c superconductivity, a description based on self-consistently solving the equations of the electron self-energy and the magnetic susceptibility in the Hubbard and tJ model. The very fact that the superconducting state emerges in high-T_c cuprates even if the doping of the initial antiferromagnetic state is relatively light probably points to the important role of fluctuations in antiferromagnetic order. A detailed study of the temperature behavior of NMR characteristics, such as the Knight shift and the spin–lattice relaxation time, in lanthanum and barium systems has shown that the detected anomalies can be explained by the presence of strong antiferromagnetic fluctuations near the wave vector $\mathbf{Q}$. Millis, Monien, and Pines [18] proposed a simple phenomenological form for the low-frequency magnetic susceptibility in $YBa_2Cu_3O_7$ that allows for a sharp enhancement of fluctuations near $\mathbf{Q}$:

$$\chi_{\mathrm{MMP}}(\mathbf{q},\omega) = \frac{\chi_{\mathbf{Q}}}{1 + \xi^2(\mathbf{q}-\mathbf{Q})^2 - \mathrm{i}\omega/\omega_s}\,. \tag{2.1}$$

Here $\chi_{\mathbf{Q}}$ is the static spin susceptibility for a wave vector $\mathbf{Q}$, ξ is the magnetic correlation length, and ω_s is the characteristic frequency of spin fluctuations. For $YBa_2Cu_3O_7$ these parameters can be found, for instance, from NMR data on ^{63}Cu, ^{17}O, and ^{89}Y nuclei, since the general theoretical relationships relating the data to the dynamic susceptibility are well-known.

The susceptibility $\chi(\mathbf{q},\omega)$ found in this manner can be used to calculate various quantities in the superconducting and normal phases of this compound, and the results of such calculations can be compared with the experimental data. In this way one can verify the main idea that the antiferromagnetic spin fluctuations are predominant.

The next step that must be taken in the phenomenological approach amounts to setting up an effective Hamiltonian. The Hamiltonian must consist of two parts: $H = H_0 + H_{\mathrm{int}}$, where $H_0 = \sum_{\mathbf{k}\sigma} \varepsilon(\mathbf{k}) C^{\dagger}_{\mathbf{k}\sigma} C_{\mathbf{k}\sigma}$ is the bare electron spectrum in the Cu–O plane, and H_{int} represents the interaction of electrons and spin fluctuations:

$$H_{\mathrm{int}} = \sum_{\mathbf{q}} g(\mathbf{q})\mathbf{s}(\mathbf{q})\mathbf{S}(-\mathbf{q})\,. \tag{2.2}$$

Here $\mathbf{s}(\mathbf{q})$ is the electron spin operator,

$$\mathbf{s}(\mathbf{q}) = \frac{1}{2}\sum_{\mathbf{k}}\sum_{\sigma\sigma'} C^{\dagger}_{\mathbf{k}+\mathbf{q}\sigma}\boldsymbol{\tau}_{\sigma\sigma'}C_{\mathbf{k}\sigma'}\,, \tag{2.3}$$

$\boldsymbol{\tau}$ represents the Pauli matrices, and $\mathbf{S}(\mathbf{q})$ is the spin fluctuation operator, whose properties are determined by the spin – spin correlation function [the dynamic susceptibility tensor $\chi_{\alpha\beta}(\mathbf{q},\omega)$]. For the paramagnetic phase $\chi_{\alpha\beta} = \delta_{\alpha\beta}\chi$. This interaction is assumed to be short-range, with the result that $g(\mathbf{q})$ in Eqn (2.2) is weakly momentum-dependent and may be set constant. We assume that $\chi(\mathbf{q},\omega)$ is given by the phenomenological expression (2.1), where the parameters are found from the NMR experimental data on the substance in question. The coupling constant remains a free parameter of the theory and can be found by calculating a quantity via the effective Hamiltonian and comparing the result with the experimental data.

Let us now examine the quantities $\chi_{\mathbf{Q}}$ and ω_{s} in Eqn (2.1). In the normal phase these quantities are given by the following expressions:

$$\chi_{\mathbf{Q}} = \chi_0\left(\frac{\xi}{a}\right)^2\beta^{1/2}\,, \qquad \omega_{\mathrm{s}} = \frac{\Gamma}{\beta^{1/2}\pi(\xi/a)^2}\,, \tag{2.4}$$

where χ_0 is the long-wavelength limit of the spin susceptibility (measured in experiments), $\beta \approx \pi^2$, and Γ is an energy constant. The NMR data on $YBa_2Cu_3O_7$ imply that

$$\xi(T_{\mathrm{c}}) \approx 2.3a\,, \qquad \omega_{\mathrm{s}}(T_{\mathrm{c}}) \approx 8\ \mathrm{meV}\,, \qquad \Gamma \approx 0.4\ \mathrm{eV}. \tag{2.5}$$

Here it is assumed that the phenomenological Hamiltonian leads to a self-consistent description of the spin behavior of the system in the sense that the spin susceptibility calculated via the effective Hamiltonian (in terms of the characteristics of the quasiclassical spectrum that, which in turn depend on the susceptibility) agrees with the values given by Eqn (2.1).

2.2 Superconductivity in the strong-coupling approximation

In the second order in the coupling constants, the interaction (2.2) of the electrons and spin fluctuations leads to the following effective electron – electron interaction:

$$V_{\mathrm{eff}} = g^2\chi(\mathbf{q},\omega)\boldsymbol{\sigma}_1\boldsymbol{\sigma}_2\,. \tag{2.6}$$

In the static limit this leads (in the coordinate representation) to the following result:

$$V_{\mathrm{eff}} \sim \exp\{\mathrm{i}\mathbf{QR}\} \sim (-1)^{R_x+R_y}\,, \tag{2.7}$$

where $\mathbf{R} = (R_x, R_y)$ is the radius vector connecting two electrons in the two-dimensional lattice. Thus, the effective interaction oscillates: at one site it is repulsive while on the adjacent sites $(0, \pm a)$ and $(\pm a, 0)$ it is attractive. On the diagonals of the square lattice $(R_x = \pm R_y)$ it is repulsive. This fact determines the symmetry of the superconducting order parameter. Obviously, the $d_{x^2-y^2}$-wave order parameter

$$\Delta(\mathbf{k}) = \Delta_0(\cos k_x - \cos k_y) \tag{2.8}$$

ensures zero values of the order parameters on the diagonals $(k_x = \pm k_y)$ of the square representing the Brillouin zone. Monthoux and Balatsky [14] set up the necessary equations for the superconductor in the weak-coupling approximation, solved these equations numerically, and found that the order parameter for model (2.2) is d-wave. To calculate the superconducting transition temperature, which for the yttrium – beryllium system amounts to 90 K, one must use the strong-coupling theory.

Let us write the Eliashberg linearized system of equations for a superconductor with the interaction of electrons and spin fluctuations given by the following expressions [16]:

$$\Sigma(\mathbf{k},\mathrm{i}\omega_n) = g^2T\sum_m\sum_{\mathbf{k}'}\chi(\mathbf{k}-\mathbf{k}',\mathrm{i}\omega_n-\mathrm{i}\omega_m)G(\mathbf{k}',\mathrm{i}\omega_m)\,, \tag{2.9}$$

$$\Phi(\mathbf{k},\mathrm{i}\omega_n) = -g^2T\sum_m\sum_{\mathbf{k}'}\chi(\mathbf{k}-\mathbf{k}',\mathrm{i}\omega_n-\mathrm{i}\omega_m)G(\mathbf{k}',\mathrm{i}\omega_m) \times G(-\mathbf{k}',-\mathrm{i}\omega_m)\Phi(\mathbf{k}',\mathrm{i}\omega_m)\,. \tag{2.10}$$

Here $\Sigma(\mathbf{k},\mathrm{i}\omega_n)$ is the self-energy of the one-particle Green's function $G(\mathbf{k},\mathrm{i}\omega_n)$ in the normal phase, and $\Phi(\mathbf{k},\mathrm{i}\omega_n)$ is the anomalous part, proportional to the superconducting order parameter. These equations combined with the Dyson equation

$$G(\mathbf{k},\mathrm{i}\omega_n) = \frac{1}{\mathrm{i}\omega_n - \varepsilon(\mathbf{k}) + \mu - \Sigma(\mathbf{k},\mathrm{i}\omega_n)} \tag{2.11}$$

produce a closed system of equations for finding the superconducting transition temperature. Here $\chi(\mathbf{q},\mathrm{i}\omega_\ell)$ is the Matsubara Green's function of spin fluctuations, which is related to the dynamic magnetic susceptibility as follows:

$$\chi(\mathbf{q},\mathrm{i}\omega_\ell) = -\int_{-\infty}^{\infty}\frac{\mathrm{d}\omega}{\pi}\,\frac{\operatorname{Im}\chi(\mathbf{q},\omega)}{\mathrm{i}\omega_\ell - \omega}\,. \tag{2.12}$$

In Eqs (2.9) – (2.11), $\omega_n = (2n+1)\pi T$ is the odd Matsubara frequency, and $\omega_\ell = 2\ell\pi T$ is the even Matsubara frequency.

Monthoux and Pines [16] used the phenomenological expression (2.1) for $\chi(\mathbf{q},\omega)$ with parameters (2.5) for $YBa_2Cu_3O_7$ and obtained the numerical solution of Eqns (2.9) – (2.11) for a single value of hole concentration, $\delta = 0.25$, and the value $t = 0.25$ for the hopping parameter, which is common for this system. They assumed that the values of the magnetic-susceptibility parameters in the yttrium – beryllium system do not change significantly under doping.

The integral equations were solved numerically on a 64×64 lattice for the wave vector and for Matsubara frequencies up to 6 eV. The transition temperature was found by solving Eqn (2.6), which is an equation for the eigenvector $\Phi(\mathbf{k},\mathrm{i}\omega_n)$. A finite solution for the superconducting order parameter emerges when the greatest eigenvalue of the matrix

$$A(\mathbf{p},\mathrm{i}\omega_n;\mathbf{q},\mathrm{i}\omega_m) = -g^2T\chi(\mathbf{p}-\mathbf{q},\mathrm{i}\omega_n-\mathrm{i}\omega_m) \times G(\mathbf{q},\mathrm{i}\omega_m)G(-\mathbf{q},-\mathrm{i}\omega_m) \tag{2.13}$$

is unity. The only free parameter in Eqns (2.9) – (2.11) is still the coupling constant g, with the result that T_{c} is calculated as a function of g. To obtain $T_{\mathrm{c}} = 90$ K, one must put $g = 1.53$.

The numerical values of T_{c} for different values of g are well approximated by the formula

$$T_{\mathrm{c}} = 0.636\,\frac{\Gamma}{\pi^2}\exp\left\{-\frac{1}{0.402N(0)g}\right\}, \tag{2.14}$$

where

$$N(0) = -\frac{2}{\pi}\sum_{\mathbf{k}} \operatorname{Im} G_R(\mathbf{k}, 0) \tag{2.15}$$

is the density of the quasiparticle states for two orientations of the spin. The retarded Green's function $G_R(\mathbf{k}, \omega)$ is obtained by analytic continuation of the Matsubara Green's function via Pade approximants [19]. We see that the expression for T_c in strong-coupling theory has the same form as the expression for the transition temperature of a superconductor with weak coupling with an effective coupling parameter $\lambda_s = 0{,}402N(0)g$, which for $YBa_2Cu_3O_{7-\delta}$ with $T_c = 90$ K is only $\lambda_s = 0.83$. The large value of the transition temperature emerges because of the large pre-exponential factor proportional to the electron parameter Γ. What is important in obtaining high values of T_c is the solution of Eqns (2.9)–(2.11) with allowance for the spin Green's function over the entire Brillouin zone (i.e. not only near the Fermi surface, which is the case in the electron–phonon model of a superconductor). We also note that the numerical solution of the linearized equation (2.10) for the anomalous self-energy part leads to a gap function $\Delta(\mathbf{k}) = \Phi(\mathbf{k}, 0)/Z(\mathbf{k}, 0)$ that is $d_{x^2-y^2}$-wave.

2.3 Quasiparticle spectrum and the physical properties of the normal phase

We can find $\Sigma(\mathbf{k}, i\omega_n)$ as a self-consistently solution of Eqns (2.9) and (2.11) for the normal phase. Using Pade approximants to analytically continue this solution, we can find the hole quasiparticle spectrum. Figure 2 depicts the imaginary and real parts of $\Sigma(\mathbf{k}, \omega)$ for a particular value of the quasimomentum on the Fermi surface. The solid curves represent the results of self-consistent calculations, while the dotted curves represent the results of calculations that allow only for first-order corrections in the coupling constant. The latter agree with the results of Kampf and Schrieffer [20]. The function $\operatorname{Re}\Sigma(\mathbf{k}, \omega)$ determines the renormalization $Z_{\mathbf{k}}$ of the quasiparticle spectrum, where $Z_{\mathbf{k}}$ varies from 0.4 to 0.6 on the Fermi surface. An analysis of the results of numerical calculations [16] shows that on the Fermi surface the function $\operatorname{Im}\Sigma(\mathbf{k}, \omega)$ varies according to the law $\alpha T + \gamma\omega^2$ within a range of frequencies not exceeding the characteristic spin-fluctuation frequency ω_s. At the same time, at high frequency there is crossover to a linear dependence on ω, a fact that is clearly visible in Fig. 2a. Thus, the system in question is a Fermi liquid, since there is a discontinuity in the particle momentum distribution and Luttinger's theorem, which states that the volume confined by the Fermi surface remains constant, holds. Here we are dealing with an antiferromagnetic Fermi liquid with remarkable properties, which manifest themselves, in particular, in the temperature dependence of the electrical conductivity and the frequency dependence of the light-induced conductivity. The latter can be calculated by the formulas

$$\sigma(\omega) = \frac{2e^2}{\hbar c}\,\bar{\sigma}(\omega)\,, \qquad \bar{\sigma}(\omega) = \frac{1}{i\hbar\omega}\left[R(\omega) - R(0)\right], \tag{2.16}$$

where the current correlation function in the approximation of loop diagrams with bare vertex parts can be expressed in terms of the electron Green's functions as follows:

$$R(i\omega_n) = -2T\sum_{\mathbf{k}\omega_m}\left(\frac{\partial\varepsilon(\mathbf{k})}{\partial k_x}\right)^2 G(\mathbf{k}, i\omega_m)G(\mathbf{k}, i\omega_m + i\omega_n) \tag{2.17}$$

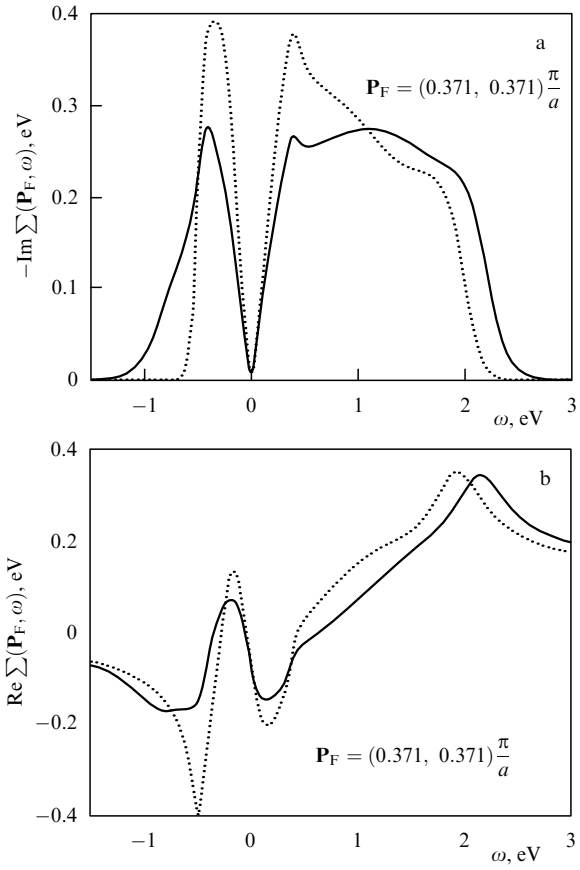

Figure 2. Imaginary and real parts of the electron self-energy for a given value of quasimomentum on the Fermi surface, $\mathbf{k}_F = (0.37, 0.37)$. Calculations were for the same values of the parameters of $YBa_2Cu_3O_{7-\delta}$ that were used in calculating $T_c = 90$ K [16].

Numerical calculations of the electrical conductivity $\rho = 1/\operatorname{Re}\sigma(0)$ at low temperatures and the parameter values adopted here lead to a linear temperature dependence $\rho = A + BT$, where $A = -28.09$ μOm cm, and $B = 1.25$ μOm cm K^{-1}. The linear temperature dependence manifests itself up to about 200 K (there are no NMR data at higher temperatures, with the result that there are no spin-susceptibility parameters).

Thus, the phenomenologically introduced spin susceptibility with parameters found from NMR in $YBa_2Cu_3O_7$ explains the existence of high-T_c superconductivity with a d-wave order parameter. At the particular value of the coupling constant $g = 1.53$ eV we have $T_c = 90$ K. The same values of the parameters ensure a quantitative description of the normal phase of this compound, e.g. the temperature dependence of the electrical conductivity and the frequency dependence of the light-induced conductivity. It was also found that the calculated value of the magnetic susceptibility is in good agreement with the value that was initially included in the calculation. Indeed, we can write the irreducible part of the susceptibility (the electron–hole loop) as

$$\tilde{\chi}(\mathbf{q}, i\omega_n) = -2T\sum_{\mathbf{k}\omega_m} G(\mathbf{k}, i\omega_m)G(\mathbf{k}+\mathbf{q}, i\omega_m + i\omega_n)\,. \tag{2.18}$$

The results of calculations of this expression in the static case are depicted in Fig. 3. Near the point $\mathbf{q} = (\pi, \pi)$ the quantity $\chi(\mathbf{q}, 0)$ has a peak, which can lead to antiferromagnetic

instability. Verifying this requires calculating the susceptibility. We seek it in the form used in RPA:

$$\chi(\mathbf{q},\omega)=\frac{\tilde{\chi}(\mathbf{q},\omega)}{1-J(\mathbf{q})\tilde{\chi}(\mathbf{q},\omega)}\,, \tag{2.19}$$

where $J(\mathbf{q})$ is the effective coupling parameter. This parameter can also be found by comparing the susceptibility calculated by Eqn (2.19) with Eqn (2.1). The results of such a comparison are depicted in Fig. 4.

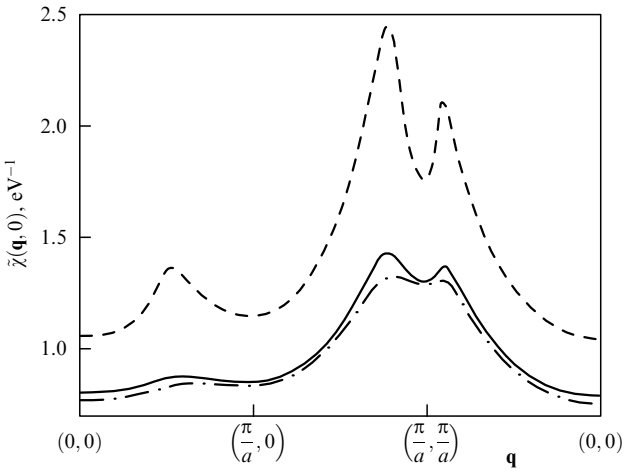

Figure 3. Irreducible part of the magnetic susceptibility calculated for free carriers (dashed curve) and for holes with a renormalized spectrum (solid curve) at $T = 90$ K [16].

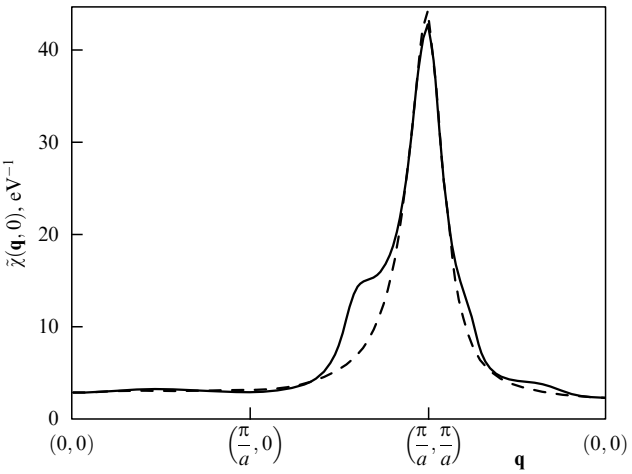

Figure 4. Magnetic susceptibility $\chi(\mathbf{q},0)$ at $T = 90$ K calculated by Eqn (2.19) (solid curve) as compared with the phenomenological expression (2.1) (dashed curve) [16].

The phenomenological magnetic susceptibility introduced in Ref. [18] was used by other researchers to study the different properties of superconductors with the spin-fluctuation pairing mechanism. For instance, Lenck and Carbotte [21] studied the equations of the BCS theory for a superconductor numerically and used Eqn (2.6) as a model of the pairing interaction. They found that the gap function $\Delta(\mathbf{k})$ has zeros, which indicated that the order parameter is d-wave, but that it differs considerably from the simple form $\Delta(\mathbf{k})$. They also calculated the penetration depth $\Delta(\mathbf{k}) \sim \sim (\cos k_x - \cos k_y)$ as a function of temperature and found that the calculated values of λ depend on the parameters of the theory, but on average exhibit a linear temperature dependence characteristic of superconductors with a d-wave order parameter (see Section 6).

Thus, the proposed phenomenological approach has made it possible to connect the properties of the normal and superconducting phases of a high-T_c compound on the basis of the dynamic susceptibility function in the form (2.1). The parameters of this function, which are determined from the NMR data of the normal phase, make it possible to obtain a correct temperature dependence of the electrical conductivity and other transport properties and to explain the large values of T_c and the nontrivial symmetry of the superconducting order parameter. The phenomenological approach reduces the problem of high-T_c compounds to the problem of microscopic calculation of the dynamic magnetic susceptibility [22]. In Sections 3 and 4 we will use the microscopic approach for the two main models of the theory of strongly correlated systems, the Hubbard model and the tJ-model.

3. The spin-fluctuation mechanism in the Hubbard model

3.1 A self-consistent system of equations for electrons and magnetic susceptibility

In the one-band models, the same electrons participate in the formation of antiferromagnetic fluctuations and in electron pairing due to the exchange of such fluctuations. This means that both the magnetic susceptibility and the electron self-energy must be calculated self-consistently. Recently, three independent groups of researchers, Lenck et al. [23], Monthoux and Scalapino [24], and Pao and Bickers [25], derived such self-consistent equations for the superconducting state and solved the equations numerically. The computational methods used by these groups differ, but the physical results are the same. In all three cases integration was over the entire $(\mathbf{k},\omega)$-space rather than only over the region near the Fermi surface (the latter approach is common for the theory of superconductors with strong coupling [5]). All three groups found that the superconducting gap function $\Delta(\mathbf{k},\omega)$, if considered a function of the quasimomentum, is $d_{x^2-y^2}$-wave and that the superconducting transition temperature $T_c \approx 0.02t$, which at parameter values characteristic of high-T_c compounds amounts to about 60 K. Below we discuss the version of Lenck et al. [23]. We begin by writing the electron energy $\Sigma(k)$ in the superconducting phase.

In the Nambu representation, the 2×2 matrix $\Sigma(k)$ is given by the following expression:

$$\Sigma(k)=\sum_{k'} V_s(k-k')\tau_0 G(k')\tau_0+\sum_{k'} V_c(k-k')\tau_3 G(k')\tau_3\,. \tag{3.1}$$

Here the τ_α ($\alpha = 0,1,2,3$) are the Pauli matrices, $G(k)$ is the electron Green's function, and V_s and V_c are the matrix elements of the electron–electron interaction due to spin and charge fluctuations:

$$V_s(q)=\frac{3}{2}\,U^2\chi_s(q)\,,\qquad V_c(q)=\frac{1}{2}\,U^2\chi_c(q)\,, \tag{3.2}$$

where $\chi_s(q)$ and $\chi_c(q)$ are the dynamic magnetic and dielectric susceptibilities.

In RPA, the two susceptibilities are given by well-known diagrams corresponding to summation of loop diagrams:

$$\chi_s(q) = \frac{\chi_{s0}(q)}{1 - U\chi_{s0}(q)}\,, \tag{3.3}$$

$$\chi_c(q) = \frac{\chi_{c0}(q)}{1 - U\chi_{c0}(q)}\,. \tag{3.4}$$

Here $\chi_{s0}(q)$ and $\chi_{c0}(q)$ are the irreducible parts, which in the single-loop approximation are given by the following formulas:

$$\chi_{s0}(q) = -\frac{1}{2}\,T\sum_k \mathrm{tr}\left\{G(k)\tau_0 G(k+q)\tau_0\right\}, \tag{3.5}$$

$$\chi_{c0}(q) = -\frac{1}{2}\,T\sum_k \mathrm{tr}\left\{G(k)\tau_3 G(k+q)\tau_3\right\}, \tag{3.6}$$

where tr stands for the trace of a two-row matrix. The Green's function $G(k)$ and the self-energy part $\Sigma(k)$ are related by the Dyson equation

$$G(k) = \left[G_0^{-1}(k) - \Sigma(k)\right]^{-1}, \tag{3.7}$$

where in the case of singlet pairing the zeroth-order Green's function is

$$G_0^{-1}(\mathbf{k}, \mathrm{i}\omega_n) = \mathrm{i}\omega_n\tau_0 - \varepsilon(\mathbf{k})\tau_3\,. \tag{3.8}$$

Here $\varepsilon(\mathbf{k})$ is the dispersion law for free electrons, which in the nearest-neighbor strong-coupling model can be written as

$$\varepsilon(\mathbf{k}) = -2t(\cos k_x + \cos k_y)\,.$$

We write the matrix $\Sigma(k)$ in standard form:

$$\Sigma(\mathbf{k}, \mathrm{i}\omega_n) = \mathrm{i}\omega_n\left[1 - Z(\mathbf{k}, \mathrm{i}\omega_n)\right]\tau_0 + \xi(\mathbf{k}, \mathrm{i}\omega_n)\tau_3 + \Phi(\mathbf{k}, \mathrm{i}\omega_n)\tau_1\,. \tag{3.9}$$

Here Z is the renormalization factor, which determines the renormalized frequency,

$$\tilde{\omega}(\mathbf{k}, \mathrm{i}\omega_n) = \omega_n Z(\mathbf{k}, \mathrm{i}\omega_n)\,, \tag{3.10}$$

$\xi(\mathbf{k}, \mathrm{i}\omega_n)$ specifies the energy shift, and the function $\Phi(\mathbf{k}, \mathrm{i}\omega_n)$ determines the superconducting gap:

$$\Delta(\mathbf{k}, \mathrm{i}\omega_n) = \frac{\Phi(\mathbf{k}, \mathrm{i}\omega_n)}{Z(\mathbf{k}, \mathrm{i}\omega_n)}\,. \tag{3.11}$$

The summation in Eqn (3.1) and subsequent equations is done over 4-momenta. The effective interaction potentials $V_s(q)$ and $V_c(q)$ depend on the difference of 4-momenta, $q = k - k'$, and are therefore defined for even frequencies.

Equations (3.1) and (3.9) simultaneously determine three coupled nonlinear equations for three quantities:

$$\tilde{\omega}(\mathbf{k}, \mathrm{i}\omega_n) = \omega_n + \sum_{\mathbf{k}'m}\left[V_s(\mathbf{k} - \mathbf{k}', \mathrm{i}\omega_n - \mathrm{i}\omega_m) + V_c(\mathbf{k} - \mathbf{k}', \mathrm{i}\omega_n - \mathrm{i}\omega_m)\right]\frac{\tilde{\omega}(\mathbf{k}', \mathrm{i}\omega_m)}{D(\mathbf{k}', \mathrm{i}\omega_m)}\,, \tag{3.12}$$

$$\xi(\mathbf{k}, \mathrm{i}\omega_n) = -T\sum_{\mathbf{k}'m}\left[V_s(\mathbf{k} - \mathbf{k}', \mathrm{i}\omega_n - \mathrm{i}\omega_m) + V_c(\mathbf{k} - \mathbf{k}', \mathrm{i}\omega_n - \mathrm{i}\omega_m)\right]\frac{\varepsilon(\mathbf{k}') + \xi(\mathbf{k}', \mathrm{i}\omega_m)}{D(\mathbf{k}', \mathrm{i}\omega_m)}\,, \tag{3.13}$$

$$\Phi(\mathbf{k}, \mathrm{i}\omega_n) = -T\sum_{\mathbf{k}'m}\left[V_s(\mathbf{k} - \mathbf{k}', \mathrm{i}\omega_n - \mathrm{i}\omega_m) + V_c(\mathbf{k} - \mathbf{k}', \mathrm{i}\omega_n - \mathrm{i}\omega_m)\right]\frac{\Phi(\mathbf{k}', \mathrm{i}\omega_m)}{D(\mathbf{k}', \mathrm{i}\omega_m)}\,, \tag{3.14}$$

where $D(k)$ is the denominator of the matrix electron Green's function:

$$D(\mathbf{k}, \mathrm{i}\omega_n) = \left[\tilde{\omega}(\mathbf{k}, \mathrm{i}\omega_n)\right]^2 + \left[\xi(\mathbf{k}, \mathrm{i}\omega_n)\right]^2 + \left[\Phi(\mathbf{k}, \mathrm{i}\omega_n)\right]^2.$$

These three equations must be augmented by an equation for the chemical potential,

$$n = \frac{1}{2} + 2T\sum_{n>0}\sum_{\mathbf{k}}\mathrm{Re}\,G_{11}(\mathbf{k}, \mathrm{i}\omega_n)\,,$$

where G_{11} is a component of the matrix Green's function G. This equation can be written in terms of the same variables as in Eqns (3.12)–(3.14):

$$n = \frac{1}{2} + 2T\sum_{n>0}\sum_{\mathbf{k}}\frac{\varepsilon(\mathbf{k}) + \xi(\mathbf{k}, \mathrm{i}\omega_n)}{D(\mathbf{k}, \mathrm{i}\omega_n)}\,. \tag{3.15}$$

Equations (3.12)–(3.15) and (3.3)–(3.6) constitute a system of self-consistent coupled equations for the electron Green's function and the dynamic susceptibilities of the superconductor and must be solved numerically for given values of the parameters t, U and n by iterations. For instance, we can plug the approximate values of the magnetic and dielectric susceptibilities into Eqns (3.12)–(3.14) and calculate the values of $\tilde{\omega}$, ξ, and Φ, which are functions that characterize the electron self-energy. Then, plugging these values into Eqns (3.3)–(3.6), we calculate new values of the susceptibilities and plug them into Eqns (3.12)–(3.14) as kernels of integral equations, which are then used to calculate new values of $\tilde{\omega}$, ξ, and Φ. This procedure is repeated many times, as long as is necessary to obtain a stable result.

3.2 Results of numerical calculations

The above procedure was carried out for a cluster of a square lattice containing 48×48 sites, which specify a discrete lattice in k-space. Also, a finite number M of Matsubara frequencies was chosen in such a way that πTM be of the order of characteristic electron energies. Thus, the problem of solving integral (in momentum and frequency) equations was reduced to the problem of solving a large number of algebraic equations, which could be solved iteratively by what is known as fast Fourier transform. The numerical solution was obtained for the following values of the external parameters:

$$t = 100\ \mathrm{meV}, \qquad U = 4.28t, \qquad n = 0.84\,. \tag{3.16}$$

Analysis has shown that a superconducting state emerges (i. e. a finite Δ emerges) at $T_c \approx 0.016t$. A complete calculation has been carried out for the temperature $T = 0.6T_c$ inside the superconducting phase.

It was found that when the parameters (3.16) are maintained, the spectrum undergoes a strong renormaliza-

tion due to the interaction of electrons and fluctuations of spin and charge. This renormalization is characterized by the parameter $Z-1$, which acts as the well-known factor λ of mass renormalization in standard superconductivity theory in the electron–phonon model, with typical values ranging from 1.5 to 2.0. At $T=0.6T_c$ the ratio of the maximum gap to T_c is large:

$$\frac{2\Delta_{\max}}{T_c}=7.7\,.$$

A remarkable result of the numerical calculations is the strong anisotropy of the gap function (Fig. 5). Within the first Brillouin zone, the positions of the negative and positive values of this functions correspond to the simple distribution provided by the function $\cos k_x-\cos k_y$.

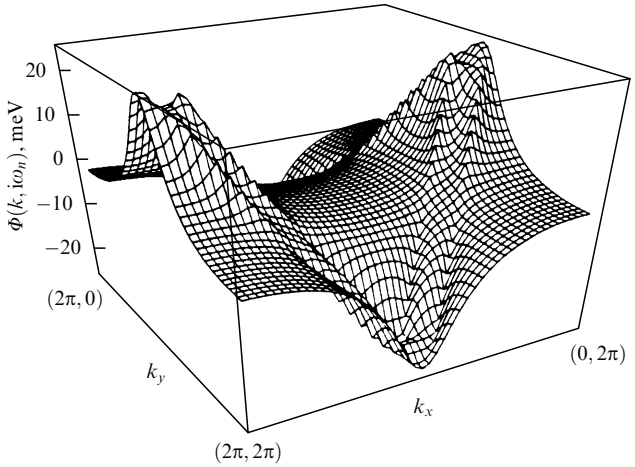

Figure 5. Gap function $\Phi(\mathbf{k}, i\omega_n)$ for $\omega_n=0$ at $T=0.6T_c$ and parameter values (3.16) [23].

The calculation of the Matsubara magnetic susceptibility $\chi(\mathbf{q}, i\omega_m)$ makes it possible to find, via an analytic continuation onto the real axis by employing the Pade approximant technique, the following quantity:

$$\lim_{\omega\to 0}\frac{\chi(\mathbf{q}, i\omega_m=\omega+i\delta)}{\omega}\,, \tag{3.17}$$

which determines the response of the system. If we consider this quantity a function of the two-dimensional wave vector, it has four sharp peaks near the point (π,π) for parameter values specified by Eqn (3.16) and $T=0.91T_c$. This suggests that there is a sharp enhancement of the magnetic susceptibility, i.e. the system is unstable with respect to formation of incommensurate phases, which implies that the chosen value $U=4.28t$ is close to the critical value $U=4.30t$ at which they begin to exhibit antiferromagnetic properties.

Thus, the numerical solution of the self-consistent equations has shown that with Eqn (3.16) for the parameter values, the Hubbard model produces a superconducting state with a d-wave order parameter and a transition temperature T_c of the order of several tens of Kelvins. Electron pairing emerges due to the interaction of electrons and spin and change fluctuations. A slight increase in U leads to antiferromagnetic ordering with a wave vector near the point (π,π). These results are in satisfactory agreement with the solution of the self-consistent equations obtained by Pao and Bickers [25], who used another method, which is conceptually close to the renormalization-group method. Compared to the method used by Lenck et al. [23], where the transition to lower temperatures is related to a large increase in the number of discrete Matsubara frequencies and hence to an increase in the number of unknowns in the algebraic system of equations, their approach made it possible to consider lower temperatures. We note, in passing, that the physical results achieved by Monthoux and Scalapino [24] (whose method is similar to that used by Lenck et al. [23]) also prove to be close. The general conclusion that can be drawn from all these studies is that the approaches used in the Hubbard model with a weak Coulomb interaction and self-consistent equations for the electron self-energy and the dynamic susceptibility in the superconductor make it possible to obtain, for a half-filled band, a solution with a d-wave order parameter and a transition temperature T_c of about 60 K for values $U\sim zt$, i.e., generally speaking, at the very limits of applicability of the method.

In conclusion of this section we would like to mention the works of Bickers et al. [26, 27], Tewordt [28], Wermbter and Tewordt [29], and Lenck et al. [30] that preceded [23–25].

4. The spin-fluctuation mechanism n the *tJ*-model

4.1 The concept of a spin polaron

The theory based on the Hubbard model proves to be insufficient for describing the superconductivity of high-T_c compounds, since its assumption is that the Coulomb interaction is weak ($U\ll W$). It is usually believed that the opposite limit ($U\gg W$) is applicable to high-T_c compounds of the metal-oxide group [31]. In this case the Hubbard model can be replaced by what is known as the *tJ*-model with the Hamiltonian

$$H=-t\sum_{ij\sigma}\tilde{C}^{\dagger}_{i\sigma}\tilde{C}_{j\sigma}+J\sum_{ij}\left(\mathbf{S}_i\mathbf{S}_j-\frac{1}{4}\,n_in_j\right), \tag{4.1}$$

where the first term on the right-hand side describes electron hops along the nearest sites of the lattice under the condition that there cannot be more than one electron at each site, and the second term describes the exchange interaction of electrons at neighboring sites with an exchange integral $J=2t^2/U$. Here $\tilde{C}^{\dagger}_{i\sigma}=C^{\dagger}_{i\sigma}(1-n_{i\bar{\sigma}})$ is the operator of electron creation under the condition that the site does not carry another electron, $\mathbf{S}_i$ is the electron spin operator,

$$\mathbf{S}_i=\frac{1}{2}\sum_{\sigma\sigma'}\tilde{C}^{\dagger}_{i\sigma}\boldsymbol{\tau}_{\sigma\sigma'}\tilde{C}_{i\sigma'}\,, \tag{4.2}$$

and n_i is the operator of the number of electrons at a single site.

The model (4.1) has been thoroughly studied for a half-filled band ($n=1$), i. e. at low hole concentrations δ (e.g. see the review article [1]). For $\delta<\delta_c$, where δ_c is the critical hole concentration, antiferromagnetic order with a wave vector $\mathbf{Q}=(\pi,\pi)$ sets in. An individual hole moves in an antiferromagnetic matrix, thus destroying the long-range order in a local region that travels together with the charge, which leads to the formation of a compound quasiparticle (the hole plus a cloud of local spin deviations). Such a quasiparticle has become known as a magnetic (or spin) polaron. Magnetic polarons form a quasiparticle band whose width is of order J. A magnetic polaron is a coherent one-particle state of the

system, and its intensity is given by the parameter $Z \sim J/t$ (the remaining intensity goes to the spectrum of incoherent states).

A magnetic polaron is formed due to the interaction of charge and spin degrees of freedom. The same interaction may lead to a superconducting pairing of quasiparticles. When the ground state is antiferromagnetic, the general model Hamiltonian (4.1) can be replaced by an effective Hamiltonian, which allows for the interaction of holes and spin waves. This is achieved by passing from the electron operators $\widetilde{C}_{i\sigma}$ and $\widetilde{C}^{\dagger}_{i\sigma}$ to the product of Fermi and spin operators (the spin–fermion representation [1]).

For two spin sublattices (denoted by $\uparrow$ and $\downarrow$) this representation has the form

$$\begin{aligned} &\widetilde{C}_{i\uparrow} = h_i^{\dagger}, \quad \widetilde{C}_{i\downarrow} = h_i^{\dagger} s_i^{+} \quad (i \in \uparrow); \\ &\widetilde{C}_{i\downarrow} = f_i^{\dagger}, \quad \widetilde{C}_{i\uparrow} = f_i^{\dagger} s_i^{-} \quad (i \in \downarrow). \end{aligned} \tag{4.3}$$

Here $h_i^{\dagger}$ and $f_i^{\dagger}$ are spinless Fermi operators producing holes at the sites of the sublattices $\uparrow$ and $\downarrow$, respectively, and s_i^{+} and s_i^{-} are spin operators. In an approximation linear in the spin waves we obtain [32]

$$\begin{aligned} H = H_0 + H_{\mathrm{int}} &= \sum_{\mathbf{q}} \omega(\mathbf{q}) \left(\alpha_{\mathbf{q}}^{\dagger}\alpha_{\mathbf{q}} + \beta_{\mathbf{q}}^{\dagger}\beta_{\mathbf{q}}\right) \\ &+ \sum_{\mathbf{kq}} h_{\mathbf{k}}^{\dagger} f_{\mathbf{k}-\mathbf{q}} \left[g(\mathbf{k},\mathbf{q})\alpha_{\mathbf{q}} + g(\mathbf{q}-\mathbf{k},\mathbf{q})\beta_{-\mathbf{q}}^{\dagger}\right] + \mathrm{c.c.} \end{aligned} \tag{4.4}$$

here $\alpha_{\mathbf{q}}^{\dagger}$ and $\beta_{\mathbf{q}}^{\dagger}$ are Bose operators of creation of spin waves with an energy $\omega_{\mathbf{q}}$, and $g(\mathbf{k},\mathbf{q})$ is the hole–spin-wave interaction amplitude,

$$\omega(\mathbf{k}) = zJs(1-\delta)^2 v(\mathbf{k}), \tag{4.5}$$

$$g(\mathbf{k},\mathbf{q}) = \frac{zt}{\sqrt{N/2}} \left(u_{\mathbf{q}}\gamma_{\mathbf{k}-\mathbf{q}} + v_{\mathbf{q}}\gamma_{\mathbf{k}}\right), \tag{4.6}$$

$$v(\mathbf{k}) = \sqrt{1-\gamma(\mathbf{k})^2}, \quad \gamma(\mathbf{k}) = \frac{1}{2}(\cos k_x + \cos k_y),$$

$$u_{\mathbf{k}} = \left(\frac{1+v(\mathbf{k})}{2v(\mathbf{k})}\right)^{1/2}, \quad v_{\mathbf{k}} = -\operatorname{sign}\gamma(\mathbf{k}) \left(\frac{1-v(\mathbf{k})}{2v(\mathbf{k})}\right)^{1/2}.$$

In contrast to ordinary polaron theory, Hamiltonian (4.4) in spin polaron theory does not contain a bare term for the holes. The quasiparticle spectrum is formed exclusively by the interaction of holes and magnetic-order fluctuations (spin waves).

Usually, when dealing with the Hamiltonian (4.4), it is common to employ the self-consistent Born approximation (SCBA). In this approximation, the quasiparticle spectrum is shown to form a narrow band whose width depends on the hole concentration, while the Fermi surface forms four pockets centered at the points $(\pm\pi/2, \pm\pi/2)$ of the Brillouin zone. The chemical potential μ depends on δ and T and can be found by solving the equation

$$\delta = \langle h_i^{\dagger} h_i \rangle + \langle f_i^{\dagger} f_i \rangle. \tag{4.7}$$

4.2 The self-consistent Born approximation for a superconductor

To employ the possibility of singlet magnetic-polaron pairing, we express (following Plakida et al. [33]) the electron Green's function in terms of the two-component operators

$$\psi_{\mathbf{k}} = \begin{pmatrix} \widetilde{C}_{\mathbf{k}\uparrow} \\ \widetilde{C}^{\dagger}_{-\mathbf{k}\downarrow} \end{pmatrix} = \begin{pmatrix} h_{\mathbf{k}}^{\dagger} \\ f_{-\mathbf{k}} \end{pmatrix},$$

$$\psi_{\mathbf{k}}^{\dagger} = \left(\widetilde{C}_{\mathbf{k}\uparrow}^{\dagger}, \widetilde{C}_{-\mathbf{k}\downarrow}\right) = \left(h_{\mathbf{k}}, f_{-\mathbf{k}}^{\dagger}\right), \tag{4.8}$$

so that the Green's function $G(k)$ and its self-energy part $\Sigma(k)$ can be represented by 2×2 matrices:

$$G(k) = \begin{pmatrix} G_{hh} & G_{hf} \\ G_{fh} & G_{ff} \end{pmatrix} = -\left\langle T\psi_k \psi_k^{\dagger} \right\rangle, \tag{4.9}$$

$$\Sigma(k) = \begin{pmatrix} \Sigma_{hh} & \Sigma_{hf} \\ \Sigma_{fh} & \Sigma_{ff} \end{pmatrix}. \tag{4.10}$$

In SCBA, the equations for the normal (Σ_{hh}) and anomalous (Σ_{hf}) parts of Σ assume the form of the Eliashberg equations:

$$\Sigma_{hh}(\mathbf{k}, \mathrm{i}\omega_n) = -T\sum_{\mathbf{q}m} G_{hh}(\mathbf{q}, \mathrm{i}\omega_m)\lambda^{11}_{\mathbf{k},\mathbf{k}-\mathbf{q}}(\mathrm{i}\omega_n - \mathrm{i}\omega_m), \tag{4.11}$$

$$\Sigma_{hf}(\mathbf{k}, \mathrm{i}\omega_n) = -T\sum_{\mathbf{q}m} G_{hf}(\mathbf{q}, \mathrm{i}\omega_m)\lambda^{12}_{\mathbf{k},\mathbf{k}-\mathbf{q}}(\mathrm{i}\omega_n - \mathrm{i}\omega_m), \tag{4.12}$$

where we have introduced the notation

$$\lambda^{11}_{\mathbf{k},\mathbf{q}}(\mathrm{i}\omega_n) = g(\mathbf{k},\mathbf{q})^2 D(\mathbf{q}, -\mathrm{i}\omega_n) + g(\mathbf{q}-\mathbf{k},\mathbf{q})^2 D(-\mathbf{q}, \mathrm{i}\omega_n),$$

$$\lambda^{12}_{\mathbf{k},\mathbf{q}}(\mathrm{i}\omega_n) = g(\mathbf{k},\mathbf{q})g(\mathbf{q}-\mathbf{k},\mathbf{q})\left[D(\mathbf{q}, -\mathrm{i}\omega_n) + D(-\mathbf{q}, \mathrm{i}\omega_n)\right]$$

for the linear combinations of the magnon Green's function $D(\mathbf{q}, -\mathrm{i}\omega_n)$. In a fully self-consistent theory there should be an equation expressing the magnon Green's function in terms of the electron Green's functions, as is done in the Hubbard model. However, in what follows we use the bare magnon Green's function with the frequency spectrum (4.5). To study T_c, we need only a system of equations linearized in the anomalous part:

$$G_{hh}(\mathbf{k}, \mathrm{i}\omega_n) = \frac{1}{\mathrm{i}\omega_n + \varepsilon(\mathbf{k}) - \mu - \Sigma_{hh}(\mathbf{k}, \mathrm{i}\omega_n)}, \tag{4.13}$$

$$\begin{aligned} \Phi(\mathbf{k}, \mathrm{i}\omega_n) = T\sum_{\mathbf{q}m} &\lambda^{12}_{\mathbf{k},\mathbf{k}-\mathbf{q}}(\mathrm{i}\omega_n - \mathrm{i}\omega_m) G_{hh}(\mathbf{q}, \mathrm{i}\omega_m) \\ &\times G_{hh}(-\mathbf{q}, -\mathrm{i}\omega_m)\Phi(\mathbf{q}, \mathrm{i}\omega_m). \end{aligned} \tag{4.14}$$

The first stage of calculating T_c consists in self-consistently calculating the normal Green's function $G_{hh}(\mathbf{k}, \mathrm{i}\omega_n)$ using Eqns (4.11) and (4.13). Here the chemical potential is found from Eqn (4.7), which assumes the form

$$\delta = \frac{1}{2} + 2T\sum_{\mathbf{k}n} G_{hh}(\mathbf{k}, \mathrm{i}\omega_n). \tag{4.15}$$

The numerical calculations were made on a lattice consisting of 64×64 points $\mathbf{k}$ in the entire Brillouin zone, and the summation over Matsubara frequencies incorporated 200 to 700 points with a cutoff at $\omega_{\max} = 10t$. Usually it was enough to do 10 to 30 iterations to obtain a solution for the self-energy with an accuracy of one part in a thousand. Calculations of the spectral density

$$A(\mathbf{k}, \omega) = -\frac{1}{\pi} \operatorname{Im} G_{hh}(\mathbf{k}, \omega)$$

of one-particle states were made by using the Pade approximant technique. The calculated quasiparticle spectrum and the Fermi surface are depicted in Fig. 6. We see that the dispersion curves have the same structure within a broad range of hole concentrations, with the energy minimum being at point S, so that the Fermi surface has four pockets centered at the points $(\pm\pi/2, \pm\pi/2)$, as shown by many researchers (see the review article [1]). Figure 6b shows that at $\delta = 0.25$ the topology of the Fermi surface may change if we include the parameter t' of next-nearest-neighbor hopping.

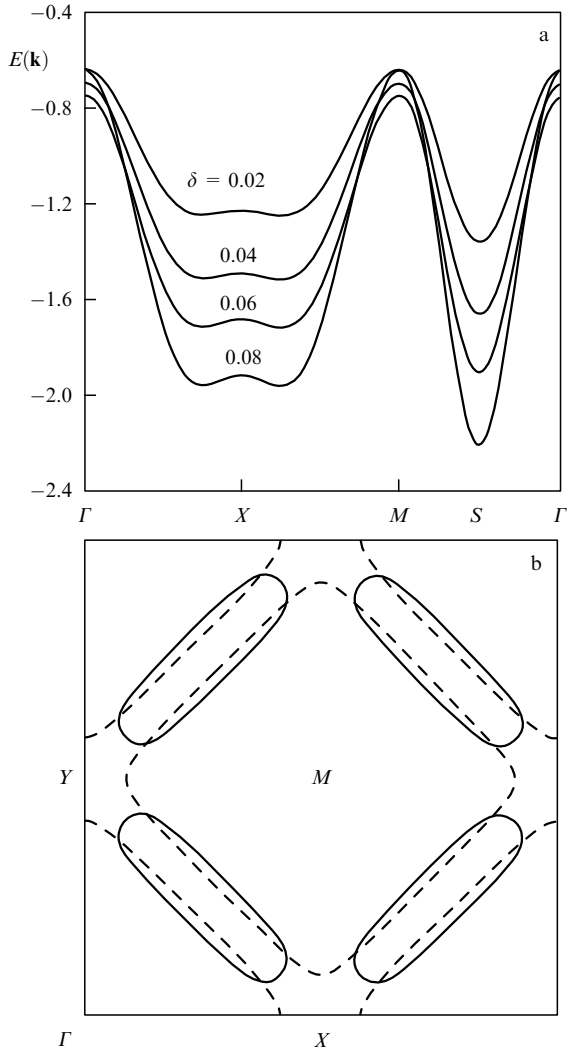

Figure 6. (a) Quasiparticle spectrum $E(\mathbf{k})$ for different hole concentrations; (b) the Fermi surface $E(\mathbf{k}_F) = 0$ for a hole concentration $\delta = 0.25$ at $J = 0.4t$ and $t' = -0.1t$. The dashed curves in Fig. 6b correspond to $t' = 0$ [33].

Figure 7 depicts the superconducting transition temperature calculated using the linearized equation (4.14) as a function of the hole concentration δ for several values of the parameter t'/t. What is remarkable is that all the curves have a peak whose position depends on t'/t. Such behavior differs significantly from other cases, where, for example, T_c monotonically increases with δ (in the weak-coupling approximation [34]) or a peak exists near concentrations for a half-filled band [35].

The solutions of Eqn (4.14) are d-waves. This also follows from the nonlinear equation (4.12), from which the superconducting order parameter $\Delta(\mathbf{k}) = \Phi(\mathbf{k}, 0)/Z(\mathbf{k}, 0)$ can be obtained as a function of the wave vector $\mathbf{k} = (k_x, k_y)$ (Fig. 8).

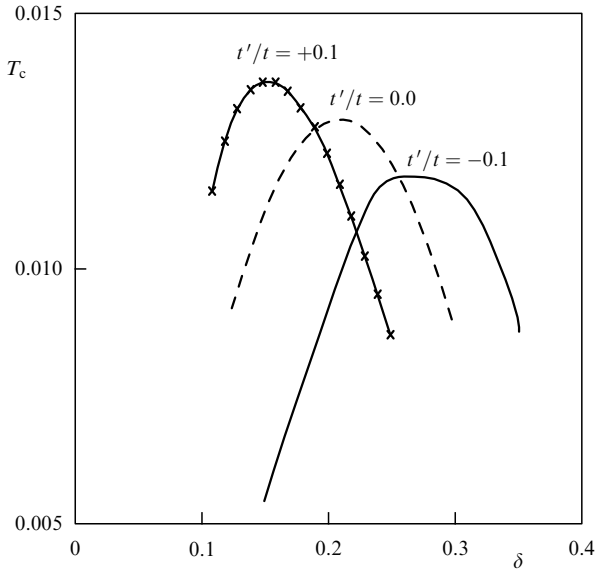

Figure 7. T_c vs. hole concentration at $J = 0.4t$ and three values of t'/t.

Several remarks concerning the above results are in order. The large values of T_c in the spin polaron model are due to a sharp peak in the density of states near the Fermi surface. In contrast to the scenario that uses a Van Hove singularity, this peak is of a multielectron nature. Here it occurs that the peak's width (the width of the polaron band) and the width of the spin-wave spectrum are of the same order J. In this situation the integration in the Eliashberg equations must be done over the entire Brillouin zone, a process that was implemented numerically.

Note, however, that attempts at comparing the results of the spin polaron theory and the properties of high-T_c systems have met with difficulties. The point is that the model Hamiltonian (4.4) was derived under the assumption that there is long-range antiferromagnetic order in the system, while superconductivity in high-T_c compounds emerges when $\delta > \delta_c$, i.e. outside a magnetically ordered state. Of course, for a large enough magnetic correlation length, the spin-fluctuation spectrum will reflect the features of the spin-wave spectrum, but without a thorough investigation it is difficult to predict the behavior of a system in which three parameters of dimension of length must be compared (i.e. the magnetic correlation length, the radius of the magnetic polaron, and the size of the Cooper pair). The cornerstone of this complicated problem is the self-consistent calculation of the spin Green's function in the absence of long-range magnetic order. The study of superconductivity within the framework of the polaron model made by Plakida et al. [33] may only be considered an attempt in building a spin-fluctuation mechanism of pairing in the tJ-model.

Let us summarize the ideas concerned in the spin-fluctuation mechanism of superconductivity discussed in Sections 2–4. We have studied three approaches to the problem, one based on the concept of phenomenological dynamic susceptibility, and two model approaches, corresponding to the limits of weak ($U \ll zt$) and strong ($U \gg zt$) Coulomb repulsion. In all three cases, large values of T_c are obtained only if we allow for integration in Eliashberg-type equations over the entire $\mathbf{k}$-space rather than only near the

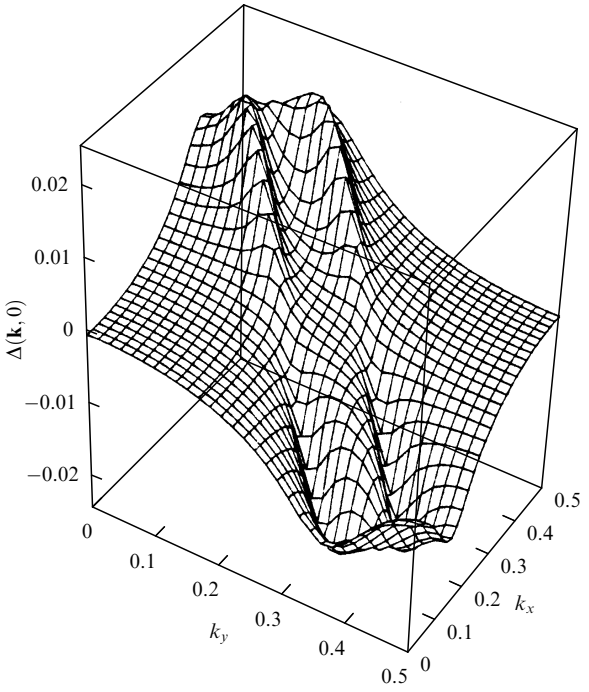

Figure 8. Superconducting order parameter $\Delta(\mathbf{k})$ at $\delta = 0.25$ and $T/T_c = 0.8$ [33].

Fermi surface. The symmetry of the order parameter in these cases automatically proves to be of $d_{x^2-y^2}$-wave type. One should not, however, overestimate this achievement of the theory, since the Eliashberg equations did not allow for the renormalization of the vertices of electron–magnon interaction, which has no such obvious smallness parameter as the adiabaticity parameter in the electron–phonon model. Another weak point of the two microscopic approaches based on the Hubbard model and the *tJ*-model is the limiting nature of the weak and strong Coulomb interaction, respectively, while it is more probable that in cuprates the intermediate case $U \sim zt$ is realized. We see, therefore, that notwithstanding the fact that some predictions of the theory of the spin-fluctuation mechanism coincide with phenomena observed in cuprates, the question of the nature of pairing in cuprates cannot be considered entirely resolved. What is most difficult in these theories is to explain the fact that many cuprates do not exhibit spin fluctuations at low energies (this follows from the experimental data on inelastic neutron scattering; e.g. see Plakida's monograph [36]), fluctuations needed for the spin-fluctuation mechanism of superconductivity to operate.

5. The Ginzburg–Landau theory for a superconductor with a d-wave order parameter

5.1 Derivation of the Ginzburg–Landau equations in the weak-coupling theory

The anisotropic spatial distribution of the superconducting order parameter in d-wave superconductors leads to a number of special features of the superconducting state in comparison to ordinary s-wave superconductors. Among these is the appearance of order-parameter zeros at the Fermi surface and the anisotropy of vortices and the structure of the vortex lattice in fields $H_{c1} < H < H_{c2}$. As is known, the behavior of type II superconductors in a magnetic field is controlled by the Ginzburg–Landau equations, which means that one must first generalize these equations for superconductors with a d-wave order parameter.

We begin with the microscopic derivation of these equations in the weak-coupling approximation [37]. The starting point is the Gor'kov equation for an inhomogeneous order parameter,

$$\Delta^*(\mathbf{r}, \mathbf{r}') = V(\mathbf{r} - \mathbf{r}')T\sum_n F^+(\mathbf{r}, \mathbf{r}'; i\omega_n)\,, \tag{5.1}$$

where $V(\mathbf{r} - \mathbf{r}')$ is the effective two-particle interaction of electrons, and F^+ is the anomalous Green's function. We denote the normal Green's function in a magnetic field by $\widetilde{G}$. The Gor'kov equations can then be written as

$$\left[i\omega_n - \frac{1}{2m}(-i\nabla + e\mathbf{A})^2 + \mu\right]\widetilde{G}(\mathbf{r}\mathbf{r}', \omega_n) + \int d\mathbf{r}''\,\Delta(\mathbf{r}\mathbf{r}'')F^+(\mathbf{r}''\mathbf{r}'; \omega_n) = \delta(\mathbf{r} - \mathbf{r}')\,, \tag{5.2}$$

$$\left[-i\omega_n - \frac{1}{2m}(i\nabla + e\mathbf{A})^2 + \mu\right]F^+(\mathbf{r}\mathbf{r}'; \omega_n) + \int d\mathbf{r}''\,\Delta^*(\mathbf{r}\mathbf{r}'')\widetilde{G}(\mathbf{r}''\mathbf{r}', \omega_n) = 0\,, \tag{5.3}$$

where $\mathbf{A}$ is the vector potential of the fields. The equations have been written for the case of a continuous medium (i.e. the discreteness of the lattice has been ignored), with result that we have a quadratic dispersion law for the electrons with an effective mass m.

Near the transition to the normal state, Eqns (5.2) and (5.3) can be solved by iterations. This leads to the appearance on the right-hand side of Eqn (5.1) of a linear term and a cubic term in Δ. The coefficients in these equations depend on the electron Green's function $\widetilde{G}_0$ in the normal phase, in which we can specify the dependence on the external field explicitly:

$$\widetilde{G}_0(\mathbf{r}\mathbf{r}', \omega_n) = \left[i\omega_n - \frac{1}{2m}(-i\nabla + e\mathbf{A})^2 + \mu\right]^{-1}\delta(\mathbf{r} - \mathbf{r}') \approx G_0(\mathbf{r}\mathbf{r}', \omega_n)\exp\{-ie\mathbf{A}(\mathbf{r})(\mathbf{r} - \mathbf{r}')\}\,. \tag{5.4}$$

This approximation holds for relatively slow variations of the magnetic field in space, when $1/k_F \ll \lambda$, with λ the London penetration depth. In Eqn (5.4), G_0 is the Green's function of free electrons in a zero field:

$$G_0(\mathbf{r}, \omega_n) = \frac{1}{(2\pi)^2}\int d\mathbf{k}\,\exp(i\mathbf{k}\mathbf{r})\,\frac{1}{i\omega_n - \xi_{\mathbf{k}}}\,, \tag{5.5}$$

where $\xi_{\mathbf{k}} = k^2/(2m) - \mu$.

Instead of using the variables $\mathbf{r}$ and $\mathbf{r}'$, it is convenient to introduce the center-of-mass radius vector $\mathbf{R} = (\mathbf{r} + \mathbf{r}')/2$ and the radius vector of relative motion, $\rho = \mathbf{r} - \mathbf{r}'$. After performing a Fourier transformation with respect to the variable $\boldsymbol{\rho}$ and using Eqn (5.5), we arrive at an equation for the superconducting order parameter $\Delta^*(\mathbf{R}, \mathbf{k})$ in the form

$$\Delta^*(\mathbf{R}, \mathbf{k}) = -\int\frac{d\mathbf{k}'}{(2\pi)^2}\,V(\mathbf{k} - \mathbf{k}')T\sum_n\frac{1}{\omega_n^2 + \xi_{\mathbf{k}'}^2}\Delta^*(\mathbf{R}, \mathbf{k}') - \int\frac{d\mathbf{k}'}{2(2\pi)^2}\,V(\mathbf{k} - \mathbf{k}')T$$

$$\times \sum_n \left[\frac{1}{(2m)^2} \frac{2\xi_{\mathbf{k}'}^2 - 6\omega_n^2}{(\omega_n^2 + \xi_{\mathbf{k}'}^2)^3} \left(k'^2_x \Pi_x^2 + k'^2_y \Pi_y^2\right) - \frac{1}{2m} \frac{\xi_{\mathbf{k}'}}{(\omega_n^2 + \xi_{\mathbf{k}'}^2)^2} \Pi^2 \right] \Delta^*(\mathbf{R}, \mathbf{k}') + \int \frac{d\mathbf{k}'}{(2\pi^2)} V(\mathbf{k} - \mathbf{k}') T \sum_n \frac{1}{(\omega_n^2 + \xi_{\mathbf{k}'}^2)^2} \left|\Delta^*(\mathbf{R}, \mathbf{k}')\right|^2 \Delta^*(\mathbf{R}, \mathbf{k}') . \quad (5.6)$$

Here $\mathbf{\Pi}_\mathbf{R} = -i\nabla_\mathbf{R} - 2e\mathbf{A}_\mathbf{R}$ is the generalized momentum. Equation (5.6) is the Ginzburg–Landau equation for the superconducting order parameter.

Now we take the effective interaction in the special form

$$V(\mathbf{k} - \mathbf{k}') = V_0 - V_1 \left[\cos(k_x - k'_x) + \cos(k_y - k'_y)\right], \quad (5.7)$$

which in the lattice model corresponds to repulsion at one site and attraction at the neighboring sites (the two constants V_0 and V_1 are positive). We write Eqn (5.7) as an expansion in the basis functions that transform according to the representations of the s-, d-, and p-symmetries:

$$V(\mathbf{k} - \mathbf{k}') = V_0 - \frac{V_1}{2} \left[\psi_\mathrm{s}(\mathbf{k})\psi_\mathrm{s}(\mathbf{k}') + \psi_\mathrm{d}(\mathbf{k})\psi_\mathrm{d}(\mathbf{k}') + \psi_\mathrm{p}(k_x)\psi_\mathrm{p}(k'_x) + \psi_\mathrm{p}(k_y)\psi_\mathrm{p}(k'_y)\right], \quad (5.8)$$

where

$$\psi_\mathrm{s}(\mathbf{k}) = \cos k_x + \cos k_y , \qquad \psi_\mathrm{d}(\mathbf{k}) = \cos k_x - \cos k_y ,$$
$$\psi_\mathrm{p}(k_\alpha) = \sin k_\alpha \qquad (\alpha = x,\ y) .$$

Here we consider only singlet pairing, so that the contribution of p-symmetry to Eqn (5.8) can be ignored. What remains of the interaction,

$$V(\mathbf{k} - \mathbf{k}') = V_\mathrm{s} - V_\mathrm{d}\psi_\mathrm{d}(\mathbf{k})\psi_\mathrm{d}(\mathbf{k}') \quad (5.9)$$

($V_\mathrm{s} = V_0 - 2V_1$ and $V_\mathrm{d} = V_1/8$), can lead to pairing of only the s- or d-type, so that we look for the superconducting order parameter in the form

$$\Delta^*(\mathbf{R}, \mathbf{k}) = \Delta_\mathrm{s}^*(\mathbf{R}) + \Delta_\mathrm{d}^*(\mathbf{R})\psi_\mathrm{d}(\mathbf{k}) . \quad (5.10)$$

Plugging this into Eqn (5.6), we arrive at a system of two coupled equations for $\Delta_\mathrm{s}^*(\mathbf{R})$ and $\Delta_\mathrm{d}^*(\mathbf{R})$:

$$2\left(1 + 2\frac{V_\mathrm{s}}{V_\mathrm{d}}\right)\Delta_\mathrm{s}^* + \alpha\lambda_\mathrm{d}\left\{\frac{1}{2} v_\mathrm{F}^2 \Pi^2 \Delta_\mathrm{s}^* + \frac{1}{4} v_\mathrm{F}^2 (\Pi_x^2 - \Pi_y^2)\Delta_\mathrm{d}^* + 2|\Delta_\mathrm{s}|^2\Delta_\mathrm{s}^* + 2|\Delta_\mathrm{d}|^2\Delta_\mathrm{s}^* + \Delta_\mathrm{d}^{*2}\Delta_\mathrm{s}\right\} = 0 , \quad (5.11)$$

$$-\lambda_\mathrm{d}\Delta_\mathrm{d}^* \ln\frac{T_\mathrm{c}}{T} + \alpha\lambda_\mathrm{d}\left\{\frac{1}{4} v_\mathrm{F}^2 \Pi^2 \Delta_\mathrm{d}^* + \frac{1}{4} v_\mathrm{F}^2 (\Pi_x^2 - \Pi_y^2)\Delta_\mathrm{s}^* + 2|\Delta_\mathrm{s}|^2\Delta_\mathrm{d}^* + \Delta_\mathrm{s}^{*2}\Delta_\mathrm{d} + \frac{3}{4}|\Delta_\mathrm{d}|^2\Delta_\mathrm{d}^*\right\} = 0 . \quad (5.12)$$

Here $\alpha = 7\zeta(3)/8(\pi T_\mathrm{c})^2$, $\lambda_\mathrm{d} = N(0)V_\mathrm{d}$, and $N(0)$ is the density of states at the Fermi surface. The transition temperature can be found from the condition that

$$\lambda_\mathrm{d} \ln\frac{2\mathrm{e}^\gamma\omega_\mathrm{D}}{\pi T_\mathrm{c}} = 1 ,$$

where ω_D is the width of a layer near the Fermi surface where there is attraction between electrons.

The s- and d-wave order parameters are coupled not only due to mixed cubic terms but also due to gradient d-wave terms. These equation must be augmented by an equation for currents obtained in the standard manner. As in ordinary superconductors, the equation for currents has the form

$$\mathbf{j}(\mathbf{R}) = -\frac{eN(0)\mu\alpha}{2m}\left\{\Delta_\mathrm{s}\mathbf{\Pi}\Delta_\mathrm{s}^* + \frac{1}{2}\Delta_\mathrm{d}\mathbf{\Pi}\Delta_\mathrm{d}^* + \frac{1}{2}(\Delta_\mathrm{s}\Pi_x\Delta_\mathrm{d}^* + \Delta_\mathrm{d}\Pi_x\Delta_\mathrm{s}^*)\mathbf{x} - \frac{1}{2}(\Delta_\mathrm{s}\Pi_y\Delta_\mathrm{d}^* + \Delta_\mathrm{d}\Pi_y\Delta_\mathrm{s}^*)\mathbf{y}\right\} + \text{c.c.} \quad (5.13)$$

($\mathbf{x}$ and $\mathbf{y}$ are basis vectors). These equations determine the vortex structure, in which the most remarkable feature is that the spatial distributions of the d- and s-components of the order parameter are different.

Note that parallel to the microscopic approach discussed here, a phenomenological approach based on an expression for the free energy written in the spirit of the original Ginzburg–Landau theory was used. Below we discuss the basics of this approach and present the results of the analysis of the Ginzburg–Landau equations in their phenomenological form [38–40].

5.2 The phenomenological approach

As for ordinary s-wave superconductors, we write the free energy for a superconductor with two order-parameter components as an expansion in powers of these components. Following the works of Berlinsky et al. [39] and Franz et al. [40], we denote these order parameters by s and d, respectively. The two order parameters are functions of coordinates and are transformed via the symmetry elements of the square lattice according to representations which in an isotropic medium correspond to orbital angular momenta $l = 0$ and $l = 2$. The expansion for the free-energy density has the form

$$f = \alpha_s|s|^2 + \alpha_d|d|^2 + \beta_1|s|^4 + \beta_2|d|^4 + \beta_3|s|^2|d|^2 + \beta_4(s^{*2}d^2 + d^{*2}s^2) + \gamma_s(\mathbf{\Pi}s)^2 + \gamma_d(\mathbf{\Pi}d)^2 + \gamma_v[(\Pi_y s)^*(\Pi_y d) - (\Pi_x s)^*(\Pi_x d) + \text{c.c.}] + \frac{h^2}{8\pi} . \quad (5.14)$$

It is assumed that d is the critical order parameter, i.e. $\alpha_d = \alpha'(T - T_d)$ and $\alpha_s = \alpha'(T - T_s)$, with $T_s < T_d$. It is also assumed that the constants β_1, β_2, β_3, β_4, γ_s and γ_d are positive, as in the ordinary theory, as is γ_v. This agrees with the results of the microscopic approach of Xu et al. [37], who also obtained an expansion for the free energy of type (5.14) with a positive coefficient of the mixed gradient term. All the parameters γ_i are related to the effective masses in the ordinary way: $\gamma_i = \hbar^2/2m_i$ $(i = s, d, v)$.

We are interested in the case where the pure d-state is stable in a massive sample in absence of inhomogeneities, i. e. in the situation where $|d| > 0$ and $s = 0$. By varying the free energy in d^* and s^* we arrive at a pair of coupled equations for the superconducting order parameter:

$$(\gamma_d\Pi^2 + \alpha_d)d + \gamma_v(\Pi_y^2 - \Pi_x^2)s + 2\beta_2|d|^2 d + \beta_3|s|^2 d + 2\beta_4 s^2 d^* = 0 , \quad (5.15)$$

$$(\gamma_s \Pi^2 + \alpha_s)s + \gamma_v(\Pi_y^2 - \Pi_x^2)d + 2\beta_1|s|^2 s + \beta_3|d|^2 s + 2\beta_4 d^2 s^* = 0\,. \tag{5.16}$$

The equation for the current can be obtained in the ordinary way, with the result that

$$\mathbf{j} = \frac{e\hbar}{2m_d}\left[d^*(\mathbf{\Pi}d) + (\mathbf{\Pi}d)^* d\right] + \frac{e\hbar}{2m_s}\left[s^*(\mathbf{\Pi}s) + (\mathbf{\Pi}s)^* s\right] - \frac{e\hbar}{2m_v}\left[s^*(\Pi_x d) + (\Pi_x s)^* d + \text{c.c.}\right]\mathbf{x} + \frac{e\hbar}{2m_v}\left[s^*(\Pi_y d) + (\Pi_y s)^* d + \text{c.c.}\right]\mathbf{y}\,. \tag{5.17}$$

Clearly, Eqns (5.15)–(5.17) of the phenomenological theory are almost equivalent to Eqns (5.11)–(5.13) of the microscopic theory. By comparing the two sets of equations we can establish the physical meaning of the phenomenological coefficients.

Equations (5.15)–(5.17) constitute the complete set of Ginzburg–Landau equations for superconductors with $d_{x^2-y^2}$-pairing. This set of equations is too complicated to analyze, so that below we consider only the most interesting particular cases — the solutions of these equations near the lower (H_{c1}) and upper (H_{c2}) critical field. In the first case the vortex number density is low, and in the second one has to deal with a vortex lattice. It occurs that the structure of an isolated vortex and the properties of a vortex lattice for d-wave superconductors differ substantially from those for ordinary s-wave superconductors [41–68]. We begin with the equations near the field H_{c1}.

5.3 The structure of an isolated vortex

Let us find the solutions of Eqns (5.15) and (5.16) when there is only one vortex and when $\lambda \gg \xi_d$. We can easily establish the asymptotic behavior of this solution in the following three regions: (1) $\mathbf{r} \to 0$, (2) $\xi_d \ll r \ll \lambda$, and (3) $r \gg \lambda$.

1. At the core of the vortex ($\mathbf{r} = 0$) both order parameters, s and d, vanish. As r increases, so does d, and this generates s and f, thanks to the mixed gradient term. At $r \approx \xi_d = \sqrt{\gamma_d/|\alpha_d|}$, the amplitude d almost coincides with its value in a homogeneous d-wave superconductor, $d_0 = \sqrt{|\alpha_d|/2\beta_2}$. At the time, s is assumed small and all s-terms in Eqn (5.15) can be ignored, with the result that this equation becomes

$$(\alpha_d + \gamma\Pi^2)d + 2\beta_2|d|^2 d = 0\,,$$

which is a well-known equation in the theory of ordinary superconductors. As $r \to 0$, the solution of this equation expressed in polar coordinates becomes

$$d(r,\varphi) = d_1 r \exp(\mathrm{i}\varphi)\,. \tag{5.18}$$

The leading term for $s(r,\varphi)$ can be obtained from the linearized equation (5.16),

$$(\alpha_s + \gamma_s\Pi^2)s + \gamma_v(\Pi_y^2 - \Pi_x^2)d = 0\,.$$

Let us calculate the result of the operator $\Pi_y^2 - \Pi_x^2$ acting on Eqn (5.18):

$$(\Pi_y^2 - \Pi_x^2)d(r,\varphi) = -\frac{eh_0}{\hbar c}\, d_1 r \exp(-\mathrm{i}\varphi)\,.$$

This leads to the following result:

$$s(r,\varphi) = s_1 r \exp(-\mathrm{i}\varphi)\,, \tag{5.19}$$

where

$$s_1 = \frac{3}{8}\left(\frac{\gamma_v}{\alpha_s \xi_d^2}\right) d_1 \ll d_1\,.$$

The most interesting feature of the solution specified by Eqns (5.18) and (5.19) is that the s- and d-components of the superconducting order parameter have opposite vorticities. This agrees with the general prediction of Volovik's symmetry analysis [41].

2. We assume that outside the core d has already reached its limit d_0, so that

$$d(r,\varphi) = d_0 \exp(\mathrm{i}\phi)\,. \tag{5.20}$$

We must now study Eqn (5.17) with this value of d and assume that $|s| \ll |d|$ and $|\nabla s| \ll |\nabla d|$. Under these two conditions the vector potential $\mathbf{A}$ can be put equal to zero and Eqn (5.16) can be replaced by the following equation:

$$\gamma_v(\partial_x^2 - \partial_y^2)d + \alpha_s s + \beta_3|d|^2 s + 2\beta_1 d^2 s^* = 0\,.$$

In terms of polar coordinates, the action of the operators on the d-functions results in

$$(\partial_x^2 - \partial_y^2)d_0 \exp(\mathrm{i}\varphi) = \frac{1}{2r^2}\left[3\exp(3\mathrm{i}\varphi) - \exp(-\mathrm{i}\varphi)\right]d_0\,,$$

so that the equation yields the following asymptotic behavior:

$$s(r,\varphi) = \frac{1}{r^2}\left[f_1 \exp(-\mathrm{i}\varphi) + f_3 \exp(3\mathrm{i}\varphi)\right], \tag{5.21}$$

where f_1 and f_3 are constants of order $f_3 \approx -3f_1 \sim \gamma_v d_0/\alpha_s$. The first to obtain the solution specified by Eqns (5.20) and (5.21) were Xu et al. [37]. In the given region, the s-component decreases as $1/r^2$, while the d-component remains constant. Here the angular dependence of the s-component is more complicated than in the core region because of the additional term $\sim \exp(3\mathrm{i}\varphi)$.

3. Finally, in the region $r \gg \lambda$ we can easily determine the exponential asymptotic behavior of the s-component of the order parameter:

$$s(r,\varphi) = \left(\frac{\pi}{2}\frac{\lambda}{r}\right)^{1/2} \exp\left(-\frac{r}{\lambda}\right)\left[s_1 \exp(-\mathrm{i}\varphi) + s_3 \exp(3\mathrm{i}\varphi)\right], \tag{5.22}$$

where $s_1 = -s_3 \sim \gamma_v d_0/2\lambda^2\alpha_s$.

Thus, at distances $r > \lambda$ the vortex has the same structure as in ordinary superconductors. At the distance $r \ll \lambda$ the d-component mixes with the s-component, which increases as $1/r^2$ as we move closer to the core but nevertheless is always smaller than the d-component. Finally, inside the core both components decrease with r (as $r \to 0$). These patterns of asymptotic behavior are corroborated by numerical solutions of the Ginzburg–Landau equations (5.15) and (5.16) (Fig. 9). The angular dependence of the singular solution of the Ginzburg–Landau equations is depicted in Figs. 9 and 10. The spatial distribution of the s-component acquires four singularities positioned around the core, and the phases of these singularities have a vorticity opposite to that of the core.

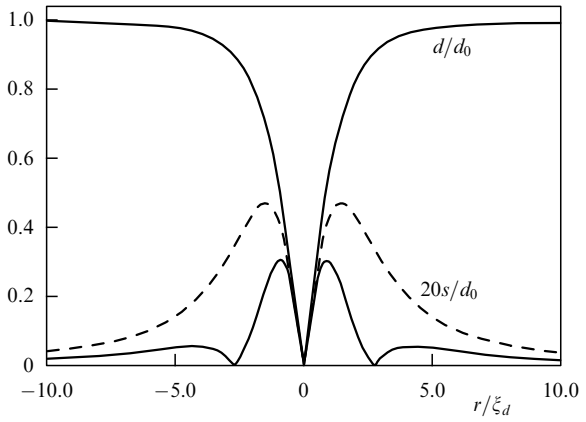

Figure 9. Amplitude of the *d*- and *s*-components of a vortex along the **x** axis (solid curve) and along the diagonal $x = y$ (dashed curve) for the following values of the parameters: $\beta_1 = \beta_3 = 0$, $\beta_4 = 0.5\beta_2$, $\alpha_3 = 10|\alpha_d|$ and $\gamma_d = \gamma_s = \gamma_v$ [40].

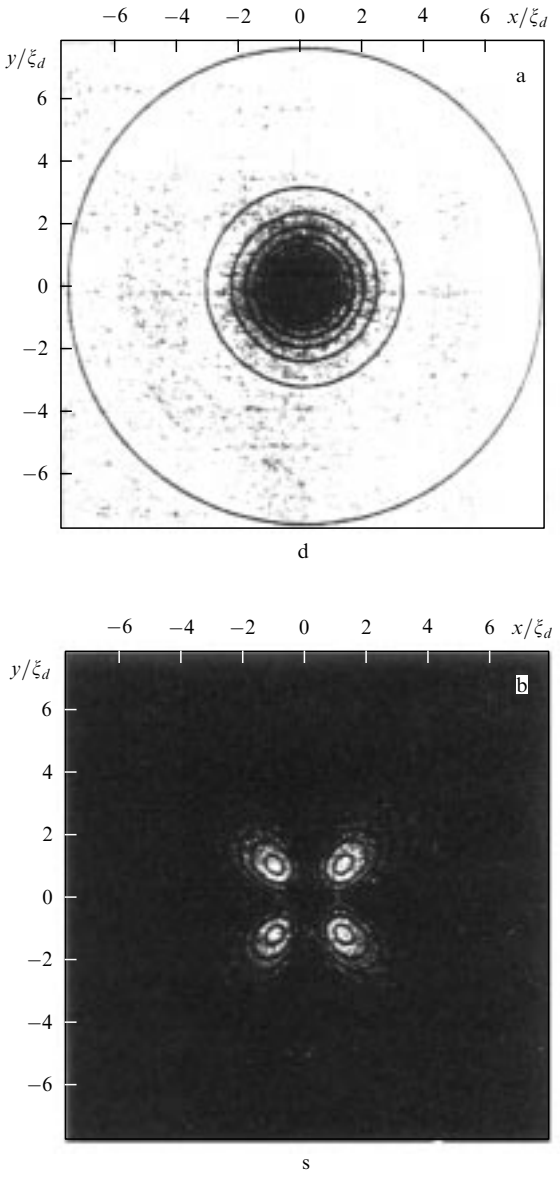

Figure 10. Contour curves of the amplitude of the *d*- and *s*-components of the order parameter for the same parameter values as in Fig. 9 [40].

What is remarkable is that the general pattern of the topological structure of the isolated vortex represented in Figs. 9 and 10 is conserved even if the free-energy parameters change.

5.4 A vortex lattice

In the vicinity of the upper critical field H_{c2}, where the vortex number density is high, the vortices form an ordered pattern in space, which is known as a vortex lattice. For d-wave superconductors, the periodic solution of the Ginzburg–Landau equations can be obtained in the same way as Abrikosov did for the first time for ordinary superconductors. The sole complicating factor here is the anisotropic distribution of the order parameter in an isolated vortex, which requires using numerical methods.

Analysis of the Ginzburg–Landau equations shows [40] that instead of a triangular lattice, which is present in ordinary superconductors, in this case we are forced to deal with an oblique vortex lattice. A characteristic feature of such a lattice is the presence of periods L_x and L_y along the corresponding directions of the initial square lattice. The measure of the obliqueness is the ratio $R = L_x/L_y$, which for a square lattice is $R = 1$, for a triangular lattice $R = \sqrt{3}$, and for an oblique lattice an intermediate value. For a given magnetic field, the equilibrium value of this ratio, $R_{\min}$, can be found by minimizing the free energy. Obviously, this parameter determines the angle θ between the shortest vectors of an oblique vortex lattice. The lattice's shape and periodicity is determined primarily by the magnetic field and an important parameter $\varepsilon_v = \gamma_v/\gamma_s$. In numerical calculations it is assumed that $\gamma_s = \gamma_d$. Figure 11 depicts an example of numerical calculations of a vortex lattice. For the specified parameter values, the shape of the lattice is characterized by $R_{\min} = 1.29$ and $\theta = 76°$. At $\varepsilon_v = 0$ the *s*-component of the order parameter vanishes and the lattice becomes triangular, as in ordinary superconductors. As ε_v increases, the lattice continuously changes its shape and becomes more and more like a square lattice.

It is possible, at least in principle, to study a vortex lattice in experiments by using small-angle neutron diffraction. Keimer [55] reported observing an oblique lattice in the YBCO system in magnetic fields $0.5T \leqslant H \leqslant 5T$, with an angle of $\theta = 73°$ between primitive translations. These observations agree with the results of calculations of Franz et al. [40], but Walker and Timusk [42] argue that the observed neutron scattering can be explained not only by the obliqueness of the lattice but also by orthorhombic distortions of the *ab*-plane. Walker and Timusk [42] report observing, by another method, an oblique lattice with $\theta = 77°$. A different method, with which the ambiguity in interpreting the results of experiments could be removed, consists in studying the lineshapes in μsR and NMR experiments.

5.5 Further development of the theory

Symmetry considerations imply (see Volovik [41]) that the $d_{x^2-y^2}$-wave order parameter contains not only an admixture of the s-wave order parameter but also order parameters of other symmetries, e.g. d_{xy}-wave. However, the coupling between $d_{x^2-y^2}$- and d_{xy}-wave order parameters is ensured not by gradient terms in the free energy that are of second order in derivatives (as in the case of the admixture of the s-wave order parameter) but gradient terms of the fourth order [43]:

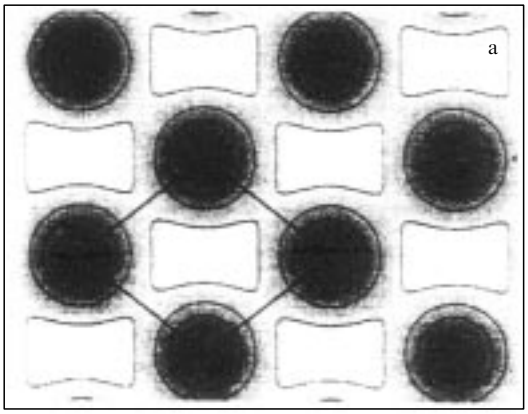

d

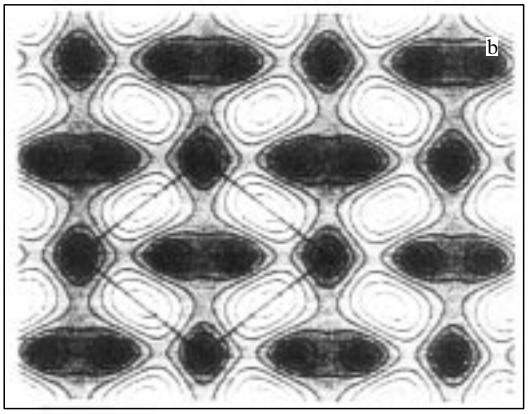

s

Figure 11. Contour curves for the altitude of an order parameter of d-type (a) and s-type (b) for a vortex lattice in a field $H = 0.8H_{c2}$ at $T = 0.75T_d$ and the following parameter values: $\beta_1 = \beta_2 = \beta_3 = \beta_4 = 1$, $\varepsilon_v = 0.45$, and $T_c = 0.5T_d$. The light areas are characterized by the highest intensity [39].

$$(\partial_x^2 - \partial_y^2) d_{x^2-y^2} \partial_x \partial_y d_{xy} \,. \tag{5.23}$$

Ichioka et al. [43] studied this situation with a semiclassical approach used earlier by Schopohl et al. [44, 45]. One advantage of this approach is that the results are valid at all temperatures, in contrast to the Ginzburg–Landau theory, which can be used only near T_c.

It was found that the accompanying order parameter changes near the core as $d_{xy} \sim r^3$, while far from the core it changes as $d_{xy} \sim 1/r^4$. The angular dependence of the order parameter is given by the formula

$$d_{xy} = d_1(r)\exp(-4i\varphi) + d_2(r)\exp(4i\varphi)\,, \tag{5.24}$$

which means that the contour map of the vortex for the d_{xy}-wave order parameter is not four-lobe (as in the case of the s-wave order parameter) but eight-lobe. The relative intensity of the accompanying component of the order parameter is determined by the value of the coefficient of the invariant (5.23) in the free energy.

Heeb et al. [46] did a detailed symmetry analysis within the Ginzburg–Landau theory for d-wave superconductors. In addition to studying the tetragonal symmetry of the initial crystal, they investigated the orthorhombic symmetry. These studies corroborated the isolated-vortex structure, earlier studied by Xu et al. [37], Soininen et al. [38], Berlinsky et al. [39], and Franz et al. [40], but the analysis took into account more thoroughly the magnetic field in the linearized Ginzburg–Landau equations. As is known, the behavior of type-II superconductors in a magnetic field is determined by the Abrikosov parameter $\varkappa = \lambda/\xi$. Heeb et al. [46] found that the approximations adopted in Refs [38–40] correspond to the $\varkappa \to \infty$ limit. But if $\varkappa$ is finite, two singularities emerge. Four satellite vortices for the s-wave order parameter move away from the center, and their intensity diminishes. The effect becomes appreciable when $\varkappa < 10$. When $\varkappa < 2$, which is close to the limit at which a type-II superconductor exists, the satellite vortices disappear completely. This explains the fact that the numerical calculations done by Xu et al. [37] (who used a microscopic approach in deriving the Ginzburg–Landau equations) did not reveal a four-lobe vortex structure, although strong anisotropy in the *s*-component of the order parameter with a fourfold symmetry axis was discovered.

In the orthorhombic phase one must allow for the mixed invariants

$$sd^*\,, \qquad (\Pi_x s)^*(\Pi_x d)\,, \qquad (\Pi_y s)^*(\Pi_y d) \tag{5.25}$$

and the complex-conjugate expressions. The invariant $sd^* + s^*d$ leads to a mixing of s- and d-wave order parameters, so that the main d-wave order parameter induces the s-wave order parameter everywhere in the bulk. This phenomenon can be detected in experiments involving Josephson junctions. For instance, Sun et al. [47] measured the tunnel current in the contact of Pb–$YBa_2Cu_3O_{7-\delta}$ with the sample surface that was perpendicular to the *c*-axis. If $YBa_2Cu_3O_{7-\delta}$ were a superconductor with a purely d-wave order parameter, the tunnel current in this contact would be zero, since in Pb the order parameter is s-wave. The induction of the *s*-component leads to a finite current, with a value determined by the fraction of the *s*-component in the order parameter for this compound. Reasoning along these lines, one can explain the origin of the current observed in the contact.

The fact that the *s*-component is finite also affects the vortex structure and, in particular, the arrangement of the satellite vortices. When the distortion of a tetragonal crystal is small, a slight displacement appears along the **x** and **y** axes in opposite directions. The gradient terms in Eqn (5.25) lead to other effects in the vortex structure. For instance, depending on the size of the distortion, six, four, two, or zero satellite vortices may appear in the *s*-component of the order parameter.

Arovas et al. [48] proposed a new type of vortex, which can realize itself in d-wave superconductors. The core of the vortex is not the paramagnetic state of a metal, as it is in an ordinary superconductor, but the antiferromagnetic state. This conclusion was reached on the basis of the theory developed in Ref. [49], which employs the SU(5) symmetry of the order parameter. In systems such as cuprates, where the antiferromagnetic state is close to the superconducting state, it is advisable to combine the three-component magnetic order parameter and the two-component superconducting order parameter (meaning its real and imaginary parts). Then the free energy can be expanded in a power series in such a five-component order parameter and the different phases and the transitions between these phases can be studied.

Note that surface states in $d_{x^2-y^2}$-wave superconductors have been studied by Walker et al. [50].

Along with the phenomenological approach to d-wave superconductors, microscopic approaches were employed [51]. For instance, Feder and Kallin [51] used the strong-coupling method to study superconductivity in two models, an extended Hubbard model proposed by Micnas and Ranninger [52] and an antiferromagnetic model with a Van Hove singularity (AvH) proposed by Dagotto et al. [53]. The first model allows from the start for repulsion between electrons at a single site and attraction between electrons at different sites. The second model allows for attraction between electrons at neighboring sites and for next-nearest-neighbor and next-next-nearest-neighbor electron hopping (there is no nearest-neighbor electron hopping). Nazarenko et al. [54] recently found that the extended model leads to instability in relation to phase stratification or to the formation of a spin density wave. Nevertheless, there is a fairly restricted region of parameter values within which a superconducting state with high T_c can exist. On the other hand, the AvH model leads to an instability in relation to d-wave superconductivity.

The Ginzburg – Landau equations have been derived for both lattice models by a technique that uses the Gor'kov equations. This means that the microscopic expressions for the phenomenological coefficients of the Ginzburg – Landau functional are known. It was found that within a broad range of values of the system parameters both models lead to a gradient coefficient ratio of order $\gamma_v/\gamma_d \sim 0.1-0.4$. This agrees with the results of recent observations [55, 56] for the vortex lattice in YBCO with angles $\theta = 73^\circ$ and 77°.

Another work worth mentioning here is that of Liu et al. [57], who used the AvH model to study the possible superposition of s- and d-wave order parameters. The problem of mixed (s + d)- or (s + id)-wave states was first investigated by Ruckenstein et al. [58] and Kotliar [59], and recently it was studied by Donovan and Carbotte [60], Ren et al. [61], and Musaelian et al. [62] in the two-dimensional model of a Fermi liquid. In the AvH model it was established that the (s + id)-phase emerges under orthorhombic distortions of a tetragonal crystal. Maki and Beal-Monod [63] derived the Ginzburg – Landau equations for an orthorhombic crystal, in which there must be a superposition of *s*- and *d*-states. The anisotropy in the *ab* plane in the normal phase is taken into account via the anisotropy of the quasiparticle effective masses. The researchers calculated the critical fields H_{c2} when an external field was applied in the base plane and perpendicular to that plane. The anisotropy in H_{c2} is accompanied by the anisotropy in penetration depth. For YBCO the calculated value $H_{c2}^b/H_{c2}^a = 3.15$ proved to be much larger than the values obtained in experiments [64]. Other research that is worth mentioning here is that of Wang and Wang [65], who derived dynamic Ginzburg – Landau equations and studied the resistance in the mixed superconducting phase, of Vicente Alvarez et al. [66], who studied the Hall effect, and of Kopnin and Volovik [67], who studied low-temperature scaling.

Won and Maki [68] and Sun et al. [47] used the microscopic approach in calculating H_{c2} and the density of states $N(0)$ on the Fermi surface in a $d_{x^2-y^2}$-wave superconductor. The structure of an isolated vortex in such a superconductor placed in a magnetic field $\mathbf{H} \parallel \mathbf{c}$ can be represented by the formula

$$\Phi_d = \cos 2\theta \left[1 + C(a^\dagger)^4 + \ldots\right] \Phi_s , \qquad (5.26)$$

where Φ_s describes the order-parameter distribution in an isolated vortex of an s-wave superconductor, and

$$a^\dagger = \frac{1}{2\sqrt{eH}} \left(-i \frac{\partial}{\partial x} - \frac{\partial}{\partial y} + 2ieHx \right) .$$

The dimensionless parameter C can be found by solving the self-consistent equations of the theory of superconductors with weak coupling. It depends on temperature approximately the same way as H_{c2}, and at $T = 0$ reaches its maximum value of 0.03. Finally, θ in Eqn (5.26) is an angle measured from the **a** axis. A microscopic calculation of $N(0)$ for a mixed superconducting state in a field $H_{c1} < H < H_{c2}$ leads to an explicit field dependence of the density of states. In fields $H_{c1} \ll H \ll H_{c2}$ the result of Won and Maki [68] transforms to Volovik's formula $N(0) \sim \sqrt{H}$ [41], which was derived in the semiclassical approximation.

6. Experimental studies of the symmetry of the superconducting order parameter

There are three groups of experiments in which the symmetry of the order parameter may manifest itself. The first group deals with measurements of various low-temperature characteristics of superconductors, such as the Knight shift and the relaxation rate in NMR, measurements of the temperature dependence of the penetration depth, and the like. If the superconducting order parameter has zeros in various sections of the Fermi surface (as it does in the $d_{x^2-y^2}$-wave case), these quantities follow a power-law temperature dependence instead of an exponential-law dependence. The second group of experiments is based on direct measurements of the order-parameter phase by studying the interference phenomena in Josephson junctions placed in a magnetic field. The third group deals with direct measurements of the gap by spectroscopic methods. The best results were achieved with ARPES, although Raman and neutron spectroscopy methods have also been used. Below we study all three groups of experiments.

6.1 Low-temperature studies of the superconducting phase

The low-temperature behavior of the various transport properties depends on the behavior of the density of states of the quasiparticle spectrum of the superconductor near the Fermi surface. The presence of zeros in the order parameter dramatically changes the function $N(\omega)$ within a narrow energy interval near ε_F, which results in the emergence of temperature anomalies in properties of the superconductor. We will study this problem using the example of the temperature dependence of the penetration depth, $\lambda(T)$ [69]. In the BCS theory this quantity is given by the relationship

$$\left[\frac{\lambda(0)}{\lambda(T)}\right]^2 = 1 - \frac{2}{T}\int_0^\infty d\omega \, \frac{N(\omega)}{N_0(0)} f(\omega)\left[1 - f(\omega)\right] , \qquad (6.1)$$

where $N_0(0)$ is the density of states at the Fermi surface in the normal phase.

For an s-wave order parameter with a constant gap Δ_0,

$$\frac{N(\omega)}{N_0(0)} = \mathrm{Re} \, \frac{\omega}{\sqrt{\omega^2 - \Delta_0^2}} .$$

In the case of a gap having zeros, at energies ω low compared to the maximum value Δ_0 we have

$$\frac{N(\omega)}{N_0(0)} \sim \frac{\omega}{\Delta_0}\,. \tag{6.2}$$

For s-wave superconductors, formula (6.1) leads at low temperatures, $T \ll \Delta_0$, to an exponentially small variation in $\lambda(T)$:

$$\frac{\lambda(T)-\lambda(0)}{\lambda(0)} \approx \left(\frac{2\pi\Delta}{T}\right)^{1/2} \exp\left(-\frac{\Delta}{T}\right).$$

However, for a $d_{x^2-y^2}$-wave superconductor, formulas (6.1) and (6.2) yield a linear temperature dependence:

$$\frac{\lambda(T)-\lambda(0)}{\lambda(0)} \approx \frac{T}{\Delta_0}\ln 2\,. \tag{6.3}$$

Figure 12 depicts the results of experimental measurements of $\lambda(T)$ for the YBCO crystal [70]. Clearly, at low temperatures the dependence on T is linear, which corroborates formula (6.3). The slope of curve is in good agreement with the numerical coefficient in Eqn (6.3) for pure YBCO (the effect of impurities will be discussed in Section 7). The linear dependence $\lambda(T)$, as a consequence of Eqn (6.2), may also occur in superconductors with an extended s-symmetry of the order parameter, so that conducting a single experiment is not enough to reliably establish whether YBCO exhibits d-wave properties. Other data are also needed so that we can distinguish between d- and s*-symmetries of the order parameter.

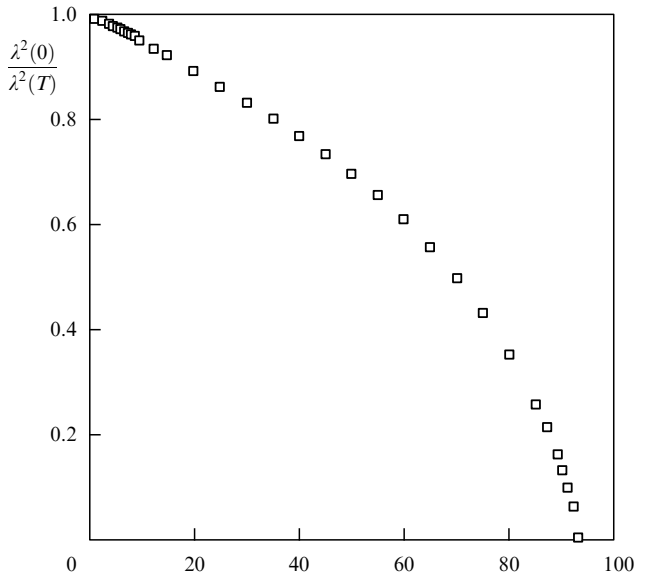

Figure 12. Microwave data on penetration depth for an $YBa_2Cu_3O_{6.95}$ crystal [69].

One experiment of this kind is an NMR experiment, in which the Knight shift K is measured as a function of temperature (Fig. 13). Qualitatively this behavior agrees with the results of the BCS theory and serves as an indication of singlet pairing in cuprates. The dashed curve represents the results of numerical calculations of K via the magnetic susceptibility for the Hubbard model in RPA [see formula (6.13)], calculated for the superconducting phase by formulas of the BCS theory under the assumption that the order parameter is d-wave [71, 72]. Similar agreement was found

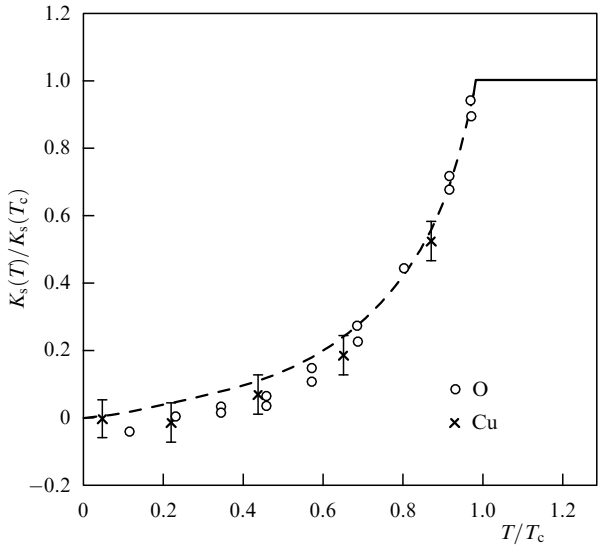

Figure 13. Temperature dependence of the Knight shift for pure $YBa_2Cu_3O_{6.95}$ determined from the behavior of oxygen and copper atoms [69].

to exist between the results of experimental observation of the NMR relaxation rate in YBCO [73] and the calculations done by Bulut and Scalapino [71, 72] under the assumption that the order parameter is d-wave. Thus, the NMR data and the experimental data on the temperature dependence of the penetration depth in the YBCO system do not contradict the $d_{x^2-y^2}$-wave nature of the order parameter. However, a direct conclusion concerning the d-wave nature of the order parameter must be made on the basis of other experiments in which the value or phase of the order parameter is measured directly.

Before describing these methods, let us briefly discuss the possibility of accessing the symmetry of the order parameter using the data on the anisotropy of the upper critical field H_{c2}. In their theoretical work, Takanaka and Kuboya [74] calculated the anisotropy of the upper critical field applied to the base plane of a tetragonal crystal, a $d_{x^2-y^2}$-wave superconductor. The anisotropy is specified by the quantity

$$\left\langle \Phi^2(\mathbf{k}) v_\perp^4 \right\rangle = A + B\cos 4\theta\,. \tag{6.4}$$

Here $\Phi(\mathbf{k}) \sim (k_x^2 - k_y^2)$ is the Cooper-pair wave function, $v_\perp$ is the electron velocity at the Fermi surface (the velocity is perpendicular to the magnetic field $\mathbf{H}$), $\langle \ldots \rangle$ stands for averaging over the Fermi surface (the surface is assumed isotropic), and θ is the angle between $\mathbf{H}$ and the crystallographic axis in the base plane. The constants A and B are expressed in terms of the averages over the Fermi surface of the product of $\Phi(\mathbf{k})$ and combinations of the fourth powers of the electron-velocity projections.

Formula (6.4) shows that H_{c2} has a fourfold symmetry axis. Hanaguri et al. [75] observed a strong anisotropy (of about 8%) of H_{c2} in the $La_{1.86}Sr_{0.14}CuO_4$ crystal with the magnetic field applied in the base plane: H_{c2} was found to have maxima in the directions $[\pm 1, 0, 0]$ and $[0, \pm 1, 0]$ and minima in the directions $[\pm 1, \pm 1, 0]$, which suggests that the order parameter is $d_{x^2-y^2}$-wave. This conclusion agrees with the data extracted from Raman spectroscopy experiments of Chen et al. [76]. Koike et al. [77] detected fourth-order anisotropy for H_{c2} in the superconductor $Pb_2Sr_2Y_{0.62}Cd_{0.38}Cu_3O_8$

using the data on the anisotropy of electrical conductivity ρ in a magnetic field for the superconductor's resistive state.

The zeros in the superconducting order parameter can manifest themselves in the field dependence of the density of states at the Fermi surface for a superconductor that is in a mixed state: $H_{c1} < H < H_{c2}$. This dependence emerges due to variations, in the magnetic field, of the electronic states within an isolated vortex line. In ordinary superconductors, the contribution of an isolated vortex to the density of states is $\sim N_0(0)\xi^2$. As shown by Volovik [41], in the case of an order parameter with lines of zeros this is $\sim N_0(0)\xi \min\{R, \lambda\}$, where R is the distance between vortices. It occurs that the main contribution is provided by the peripheral regions of the vortex, that is, for r's satisfying the conditions $\xi \ll r \ll \min\{R, \lambda\}$. For a vortex lattice in the range $H_{c1} < H < H_{c2}$, $R \sim \xi\sqrt{H_{c2}/H} < \lambda$, with the result that the density of states averaged over the vortices is given by the formula

$$\delta N(0) = CN_0(0)\sqrt{\frac{H}{H_{c2}}}, \tag{6.5}$$

where C is a quantity of value unity. Measurements of the low-temperature specific heat in $YBa_2Cu_3O_{6.95}$ have shown that the coefficient γ of the linear term in the specific heat depends on the field as $\sqrt{H}$. This is one more confirmation that in this superconductor the order parameter has zeros at the Fermi surface.

6.2 Measurements of the Josephson tunnel current

The most detailed information about the symmetry of a superconducting order parameter can be extracted from the phase of the order parameter by measuring the critical current in Josephson junctions placed in a magnetic field. In the standard rectangular geometry of junctions, the critical current oscillates with the field according to the law of Fraunhofer diffraction,

$$I_c(\Phi) = J_0 A \frac{\sin(\pi\Phi/\Phi_0)}{\pi\Phi/\Phi_0}, \tag{6.6}$$

where Φ is the magnetic flux through the junction, $\Phi_0 = hc/2e$ is the quantum of magnetic flux, J_0 is the critical-current density in a zero field, and A is the junction's surface area. The diffraction pattern is depicted in Fig. 14a.

Let us assume that we have a crystal with tetragonal symmetry, say, the superconductor YBCO. Suppose that its c axis points in the direction perpendicular to the plane of the figure. In a tunneling junction of angular geometry, the superconductor touches both faces of the first superconductor perpendicular to a and b, so that the two superconductors are in contact (Figs. 14b and c). In this case we have a superposition of the tunnel currents generated by the motion of electrons with wave vectors k_x and k_y, so that the resulting diffraction pattern depends on the symmetry of the order parameter being investigated. For the s-wave case (including the anisotropic case), the order parameters on both edges of the angular junction coincide, and the resulting diffraction pattern is the same as in the case of a standard junction. But if we are dealing with the $d_{x^2-y^2}$-wave case, the order parameters on the two edges of the angular junction have opposite signs, which radically changes the diffraction pattern. The superposition of two tunnel currents leads to an entirely different pattern (Fig. 14c). In a zero field the critical current proves to

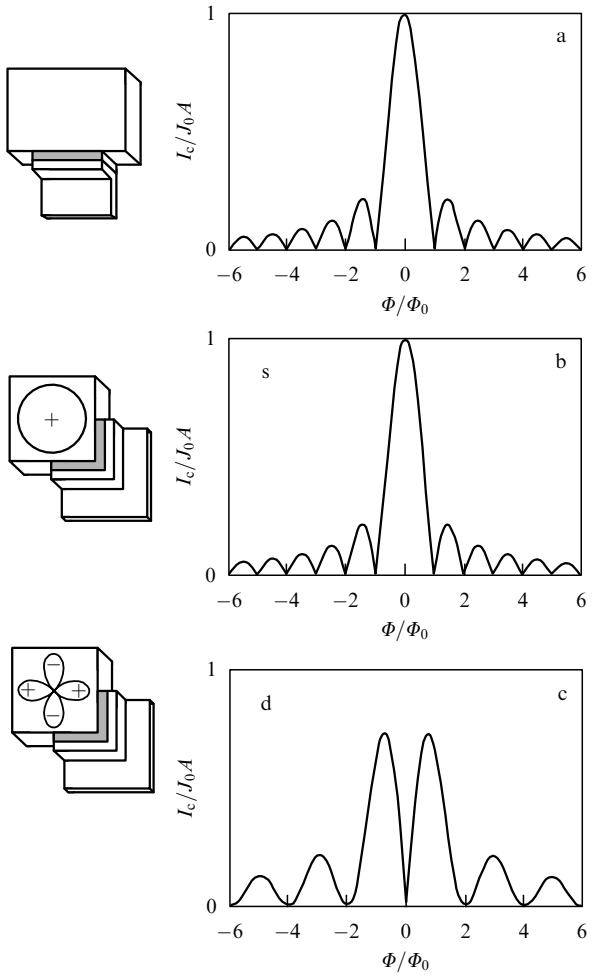

Figure 14. Critical current in a Josephson junction as a function of the applied magnetic field: (a) standard tunnel junction, (b) angular tunnel junction for a superconductor with an s-wave order parameter, and (c) angular tunnel junction for a superconductor with a $d_{x^2-y^2}$-wave order parameter [79].

be zero because of the perfect balance of its two components. In a symmetric junction (the dimensions of the junctions at the edges a and b are the same), the field dependence is given by the formula [79]

$$I_c(\Phi) = J_0 A \frac{\sin^2(\pi\Phi/2\Phi_0)}{\pi\Phi/2\Phi_0}, \tag{6.7}$$

reflected by the pattern in Fig. 14c.

Wollman et al. [79, 80] carried out such an experiment involving the tunneling junction YBCO – Au – Pb. The results of their experiment, depicted in Fig. 15, suggest that the order parameter in the superconductor YBCO is $d_{x^2-y^2}$-wave.

All the experiments with Josephson junctions mentioned above used the single crystal $YBa_2Cu_3O_{6.6}$. Brawner and Ott [81] studied another single crystal, $YBa_2Cu_3O_{6.9}$, enriched with oxygen. The results of measurements of the critical current in Josephson junctions with an angular geometry corroborate the diffraction pattern in Fig. 14c.

Other experiments in measuring the tunnel current between two superconductors with a different boundary geometry have also been proposed [82]. The results of these measurements do not agree with the d-wave nature of the order parameter. Other studies worth noting are those of Sun

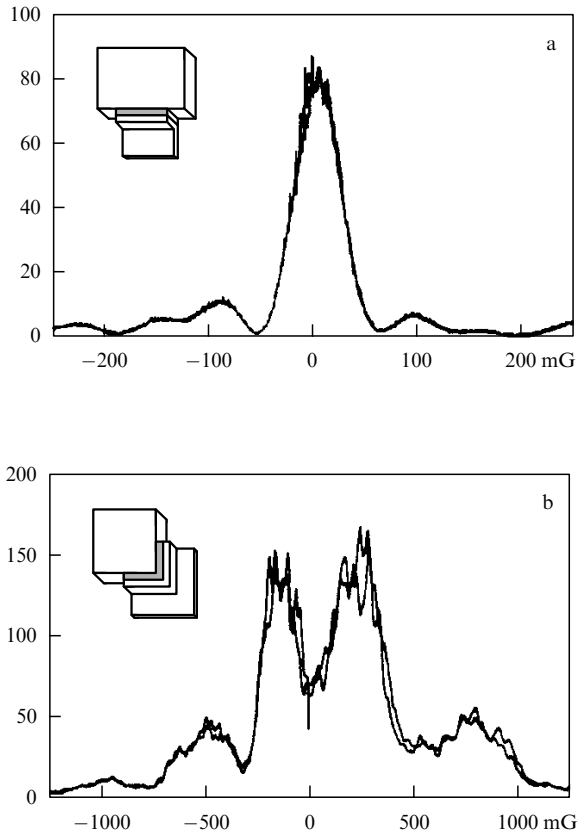

Figure 15. Critical current as a function of the magnetic field in the Josephson junction YBCO–Au–Pb in two geometries: (a) standard, and (b) angular [79].

et al. [83] and Kleiner et al. [84], who examined the Josephson junction between ordinary superconducting Pb and YBCO, with the c axis of the latter pointing in the direction perpendicular to the junction. The tunnel current generated in the junction proved to be approximately ten times weaker than the current in the standard-geometry junction. If the order parameter in the crystal were $d_{x^2-y^2}$-wave, there would be no current along the c axis. The fact that such a current exists can be explained if we assume that the crystal is orthorhombic rather than tetragonal. In this case there is an admixture of the s-component of the order parameter to the main d-component, and this ensures that the tunnel current is finite [85]. A detailed theoretical analysis of experiments with Josephson junctions in this geometry was done by Kirtley et al. [86].

Other variants of tunnel experiments involving the YBCO system in a magnetic field were carried out by Miller et al. [87] and Mathai et al. [88]. Their results agree with the assumption that the order parameter in such a system is $d_{x^2-y^2}$-wave. Recently, in their fundamental work, Tanaka and Kashiwaya [89] built a complete theory that describes the flow of a Josephson current between two superconductors separated by an insulator. They derived a general formula for the current, and all results described in the literature prove to be particular cases of this formula. Along with the case of junctions between s-wave and d-wave superconductors, they studied the Josephson current flowing between two superconductors with the d-wave order parameter.

It occurs that the magnetic current has an anomalous temperature dependence in relation to s–s and s–d superconducting pairs in the junction. The current in a d–d pair exhibits different properties, and this fact can be used to determine the symmetry of the order parameter. Tanaka and Kashiwaya [89] have provided a complete list of the experimental and theoretical papers that deal with the problem of Josephson junctions between superconductors with anomalous order parameters. The most recent experimental studies of Josephson junctions in cuprates are discussed in [90].

6.3 Measurements of flux quantization by tricrystal devices

Another type of experiment in which the symmetry of the order parameter is determined is based on measurements of the quantum of magnetic flux in a superconducting ring with specially designed Josephson junctions. The idea of such an experiment is based on the theoretical result of Sigrist and Rice [91], who found that in the case of $d_{x^2-y^2}$-wave superconductors the tunnel current between two superconducting crystals separated by a thin boundary depends on the orientation of the order parameter (the Cooper-pair wave function) in relation to the boundary. The current between the ith and jth superconductors is given by the formula

$$I_s^{ij} = (A^{ij} \cos 2\theta_i \cos 2\theta_j) \sin \Delta\Phi_{ij} . \tag{6.8}$$

Here A^{ij} is a constant characterizing the ij-junction, θ_i and θ_j are the angles between the crystallographic axes and the boundary plane, and $\Delta\Phi_{ij}$ is the phase difference of the order parameters on both sides of the boundary.

Sigrist and Rice [91] also found that if there is a superconducting ring with a single Josephson junction and a phase difference π, spontaneous magnetization corresponding to half of Φ_0 sets in. More than that, if the ring has an odd number of π-junctions, the results is the same. The discovery of a half-quantum of the magnetic flux passing through such a ring would suggest that the order parameter is d-wave. Tsuei et al. [92] conducted such an experiment. They used superconducting YBCO junctions with zero, two, and three boundary Josephson junctions. The geometry of their experiment is depicted in Fig. 16. YBCO rings were prepared on the substrate of an epitaxial film $SrTiO_3$, manufactured as three single crystals, which form rectangular boundaries. The a and b axes of the tetragonal crystals $SrTiO_3$ lie in the plane of the figure. YBCO, in which the a and b axes coincide with the substrate axes, is epitaxially grown on the crystalline substrate. Thus, the superconducting rings are crystallographically oriented in different sectors of the substrate as shown in Fig. 16. Calculations by Eqn (6.8) show that the central ring with three boundaries has a π-junction, and this ring can trap a half-integral number of quanta of magnetic flux, i.e. $\Phi = (n + 1/2)\Phi_0$.

The field strength in the ring was measured by a SQUID microscope with a 10-μm measuring loop. A series of measurements of the trapped flux was conducted in each superconducting ring at temperatures ranging from slightly above T_c ($T_c = 90$ K) down to 4.2 K. It was found that the difference of fluxes trapped in the third and second (or zeroth) rings always constitutes a half-integral value of Φ_0. The details of this experiment can be found in Refs [92–94]. Kirtley et al. [94] discussed a similar experiment with a thallium superconductor Tl2201. A detailed theoretical analysis of the potential of the tricrystal Josephson technique was carried out in a recent paper by Samanta and Datta [95].

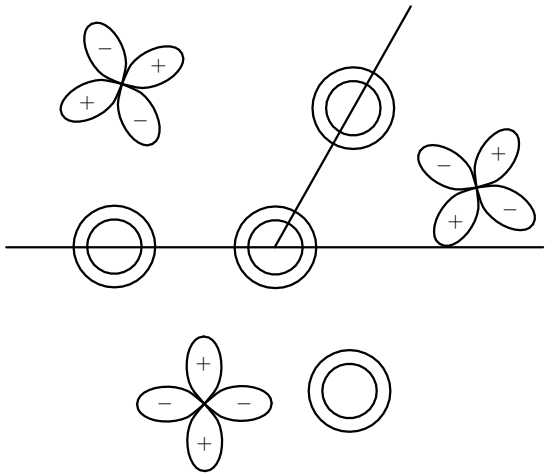

Figure 16. Geometry of an experiment that makes it possible to measure a half-integral number of quanta of magnetic flux trapped by a superconducting ring with three Josephson junctions with a d-wave order parameter [94].

6.4 Angle-resolved spectroscopy

Angle-resolved photoemission spectroscopy (ARPES) makes it possible to measure the gap in different segments of the Fermi surface. The intensity of the emitted photons, generated by the X-rays of electrons knocked out from the inner atomic shells, is proportional to $f(\omega)A(\mathbf{k},\omega)$, where $f(\omega)$ is the Fermi function, and $A(\mathbf{k},\omega)$ is the spectral density of quasiparticles of energy ω and quasimomentum $\mathbf{k}$. The edge in the energy distribution of photons determines the Fermi level. In the superconducting state, the spectral density of quasiparticles in the BCS theory is given by the formula

$$A(\mathbf{k},\omega) = u_{\mathbf{k}}^2 \frac{\Gamma/\pi}{\big(\omega - E(\mathbf{k})\big)^2 + \Gamma^2} + v_{\mathbf{k}}^2 \frac{\Gamma/\pi}{\big(\omega + E(\mathbf{k})\big)^2 + \Gamma^2}\,, \tag{6.9}$$

where $E(\mathbf{k}) = \big[(\varepsilon(\mathbf{k}) - \mu)^2 + \Delta_{\mathbf{k}}^2\big]^{1/2}$ is the quasiparticle energy, and Γ is the damping (we assume it to be independent of $\mathbf{k}$), $\Delta_{\mathbf{k}}$ is the superconducting gap, and $v_{\mathbf{k}}^2 = 1 - u_{\mathbf{k}}^2 = \big[1 - \varepsilon(\mathbf{k})/E(\mathbf{k})\big]/2$. On the Fermi surface $E(\mathbf{k}) = \Delta_{\mathbf{k}}$, so that the energy distribution of the photons exhibits a peak, whose position is determined by the size of $\Delta_{\mathbf{k}}$. The photoemission spectrum from the superconducting sample is formed at two temperatures, only slightly higher than T_c and at low temperatures, at which the gap is at its maximum. The shift of the edge of the spectrum as T lowers is determined by the size of the gap.

Detailed ARPES experiments have been conducted with $Bi_2Sr_2CaCu_2O_8$ crystal (Bi2212 in concise notation) [96–100]. Typical spectroscopic data are depicted in Fig. 17. For the wave vector $\mathbf{k}_A$ a shift on the emission edge under cooling is clearly visible, while for $\mathbf{k}_B$ no such shift has been recorded. These data point to a strong anisotropy of the gap. Further studies clearly showed that there are points at the two-dimensional Fermi surface where the gap vanishes (Fig. 18). A good description of the behavior of the gap in $\mathbf{k}$-space is provided by the function $\Delta_{\mathbf{k}} \sim (\cos k_x - \cos k_y)$, which suggests that the order parameter is $d_{x^2-y^2}$-wave. ARPES is a powerful method of studying not only the superconducting properties of a metal but also the electron characteristics of the metal's normal phase. For instance, for the Bi2212 system

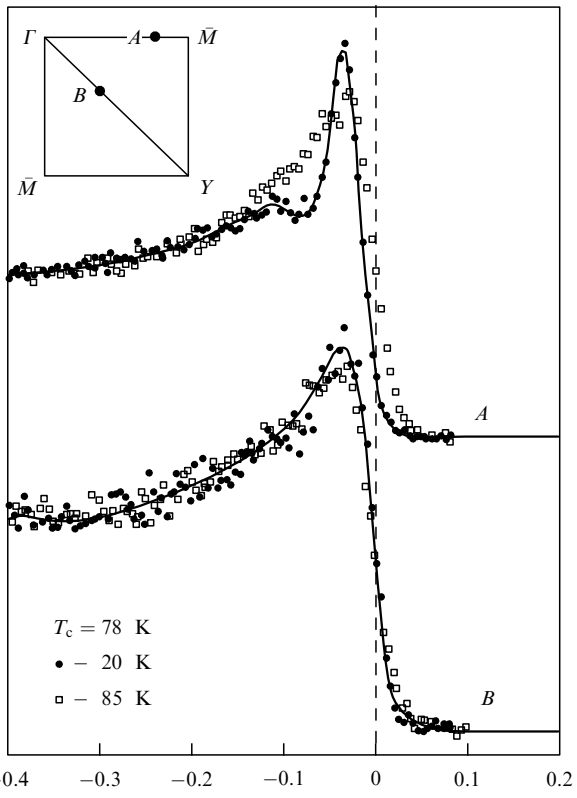

Figure 17. ARPES data for the Bi2212 crystal above and below $T_c = 79$ K for two points (A and B) on the Fermi surface [96].

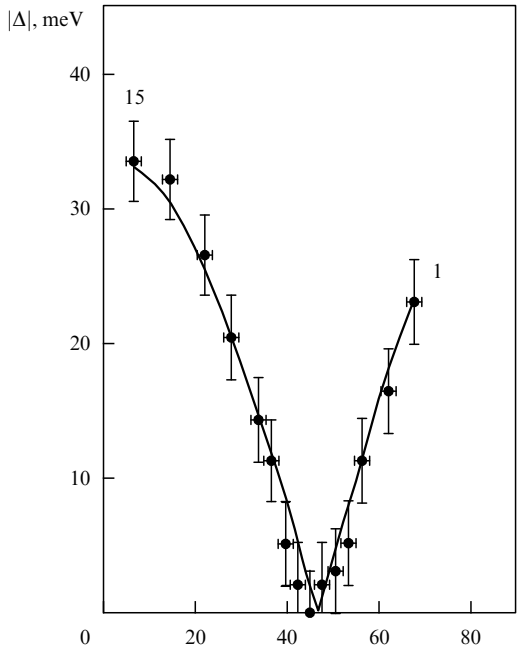

Figure 18. Gap $\Delta(\mathbf{k})$ as a function of the angle determining the deviation of vector $\mathbf{k}$ from the direction ΓY for the Bi2212 superconductor.

the various properties of the quasiparticle spectrum and the Fermi surface have recently been studied by Ding et al. [101].

6.5 Raman and neutron spectroscopy

Information about the symmetry of the superconducting gap can be extracted from experiments in inelastic scattering of

light or neutrons by electronic excitations. The Raman spectrum emerges when light is scattered by electronic excitations near the Fermi surface. Of interest here is the transformation of the observed spectrum of the superconductor when the temperature drops below T_c, a transformation that is due to the appearance of a gap in the electron energy. The dependence of the cross section of scattering of light by quasiparticles in a superconducting metal is given by the formula [102]

$$\frac{d^2R}{d\omega d\Omega} = \frac{4N(0)r_0^2}{\omega}\left\langle \frac{|\gamma(\mathbf{k})|^2|\Delta_{\mathbf{k}}|^2}{(\omega^2-4|\Delta_{\mathbf{k}}|^2)^{1/2}}\right\rangle_{S_F}. \tag{6.10}$$

Here $r_0 = e^2/mc^2$ is the electromagnetic radius of the electron, $\gamma(\mathbf{k})$ is the matrix element of the electron Raman scattering, and $\langle \ldots \rangle_{S_F}$ stands for averaging the wave vector $\mathbf{k}$ over the Fermi surface. Equation (6.10) is valid in the limit where $\lambda \gg \xi$, i.e. for short scattering vectors, $\mathbf{q} \to \mathbf{0}$. In the nonresonance limit, the tensor $\gamma(\mathbf{k})$ is given by the formula

$$\gamma_{\alpha\beta}(\mathbf{k}) = \frac{m}{\hbar^2} e_\alpha \frac{\partial^2 \varepsilon(\mathbf{k})}{\partial k_\alpha \partial k_\beta} e'_\beta, \tag{6.11}$$

where e_α and e'_β are the components of the polarization vector of the incident and scattered photon beams. In contrast to the case of ordinary s-wave superconductors, where there is no scattering for $\omega < 2\Delta$, in superconductors with an anisotropic gap there can be scattering at frequencies much lower than Δ.

Equations (6.10) and (6.11) make it possible to examine the gap behavior as a function of the wave vector, $\Delta(\mathbf{k})$, in experiments. Selecting e_α and e'_β in accordance with the geometry of the experiment, one chooses [in the general expression (6.10)] separate segments of the Fermi surface and finds the gap size in these segments. This yields information about the anisotropy of $\Delta_{\mathbf{k}}$. For instance, we can select e_α and e'_β in such a way that $\gamma(\mathbf{k})^2$ transforms as $k_x^2 - k_y^2$ or as $k_x k_y$. In these cases Eqn (6.10) yields different functions of ω for $d_{x^2-y^2}$-, d_{xy}- and s-symmetries.

Devereaux et al. [103] studied the Raman spectra of the superconductor $Bi_2Sr_2CaCu_2O_8$. The theoretical analysis of the polarization dependence of the spectrum intensities and the way in which this spectrum varied with temperature as the sample was cooled from $T > T_c$ to a low temperature suggested that the order parameter is $d_{x^2-y^2}$-wave. However, Krantz and Cardona [104] disagreed and argued that the presented experimental data were insufficient to distinguish between $d_{x^2-y^2}$-wave and extended s-wave order parameters in the superconductor in question. Continuation of the discussion has not resolved the issue (see Ref. [105]).

Chen et al. [76] measured the low-energy Raman spectrum in the single crystal $La_{1.83}Sr_{0.17}CuO_4$ at temperatures above and below T_c. They discovered a redistribution of intensities resulting from the appearance of a finite superconducting gap. By analyzing the dependence of intensity on photon polarization they found that the gap is anisotropic and has zeros along the directions $[\pm 1, \pm 1]$ and maxima along the directions $[0, \pm 1]$ and $[\pm 1, 0]$. This suggests that the order parameter is $d_{x^2-y^2}$-wave. The maximum value of the gap is related to T_c by the formula $2|\Delta_{max}| \approx 7.7T_c$. The behavior of Raman spectra in the lanthanum system is similar to that observed in the low-oxide superconductors YBCO [106] and Bi2212 [103].

Further theoretical studies of the Raman spectra, which allowed for electron screening [107], revealed the worse agreement with the experimental data for the superconductor YBCO. All this implies that although Raman spectroscopy does provide a method for establishing the symmetry of the order parameter of a superconductor, there is still not enough convincing evidence for cuprates [108, 109].

Many experiments have been conducted using optimally doped YBCO compounds. Today, however, the focus is on underdoped and overdoped substances. ARPES experiments [110–113] involving underdoped compounds have revealed that the Fermi surfaces of such compounds have segments near $(\pm\pi, 0)$ and $(0, \pm\pi)$ where the spectral intensity is much lower than it is for doped compounds. Additional information was obtained in a Raman scattering experiment with the compound $YBa_2Cu_3O_{6.5}$ ($T_c = 61$ K) [114], which showed that the low-temperature spectra have zeros near the directions $[\pm 1, \pm 1]$ in $\mathbf{k}$-space. What was also recorded was a significant reduction in the spectral intensities in the same segments as in ARPES experiments. The observed change in the spectra at $T > T_c$ and in the superconducting phase and the comparison of the spectra with those in optimally doped compounds led Marshall et al. [110], Loeser [111], Ding et al. [112, 113], and Chen et al. [114] to the conclusion that this reduction in spectral intensity of the quasiparticles in the segments of the Fermi surface near $(\pm\pi, 0)$ and $(0, \pm\pi)$ is due to the opening of a $d_{x^2-y^2}$-wave normal pseudogap in these segments. The possible mechanisms of pseudogap formation were discussed by Kivelson and Emery [115] and Wen and Lee [116], although they did not arrive at a definite theoretical explanation of this phenomenon.

In recent years there have been many experimental studies of spin fluctuations in copper-oxide cuprates by neutron spectroscopy methods. Since these methods require rather large single crystals, neutron studies have been limited to LSCO [117, 118] or YBCO [119] type superconductors. In the latter case there is no low-frequency fluctuation spectrum, but in the lanthanum system fluctuations have been observed in the normal phase ($T = 40$ K); however, their strength rapidly decreases in the superconducting phase ($T = 4$ K) at $\omega = 3.5$ meV. This quantity must be identified with the superconducting gap. The size of this gap and the value $T_c = 37$ K are in qualitative agreement with the fact that the order parameter is of the $d_{x^2-y^2}$-wave type, although the experiments do not make it possible to directly observe the effects associated precisely with a d-wave order parameter. There is a method developed by Lu [120] for observing the type of nonstandard superconducting order parameter by employing the data on the $\mathbf{q}$-dependence of the dynamic structure factor $S(\mathbf{q}, \omega)$, which can be found from inelastic neutron scattering studies. It occurs that for a superconductor whose order parameter has zeros, the dynamic structure factor exhibits peaks at low temperatures and large scattering vectors $\mathbf{q}$. These peaks are high when the energy transfer ω is much smaller than the maximum value of the superconducting gap $\Delta_{\mathbf{k}}$.

The structure factor $S(\mathbf{q}, \omega)$ corresponding to magnetic neutron scattering can be expressed in terms of the imaginary part of the dynamic susceptibility:

$$S(\mathbf{q}, \omega) = [1 + n(\omega)]\, \mathrm{Im}\, \chi(\mathbf{q}, \omega), \tag{6.12}$$

where $n(\omega)$ is the Bose distribution function. To detect the above-mentioned anomalies in $S(\mathbf{q}, \omega)$ it is enough to study $\chi_0(\mathbf{q}, \omega)$, which is the dynamic susceptibility in the single-loop approximation. This function can be expressed in terms of the Lindhard function, which in the BCS theory is given by the following formula:

$$\chi_0(\mathbf{q},\omega)=\sum_{\mathbf{k}}\frac{1}{2}\left[1+\frac{\xi(\mathbf{k}+\mathbf{q})\xi(\mathbf{k})+\Delta(\mathbf{k}+\mathbf{q})\Delta(\mathbf{k})}{E(\mathbf{k}+\mathbf{q})E(\mathbf{k})}\right]\times\frac{f\bigl[E(\mathbf{k}+\mathbf{q})\bigr]-f\bigl[E(\mathbf{k})\bigr]}{\omega-\bigl[E(\mathbf{k}+\mathbf{q})-E(\mathbf{k})\bigr]+\mathrm{i}\Gamma}+\sum_{\mathbf{k}}\frac{1}{4}\left[1-\frac{\xi(\mathbf{k}+\mathbf{q})\xi(\mathbf{k})+\Delta(\mathbf{k}+\mathbf{q})\Delta(\mathbf{k})}{E(\mathbf{k}+\mathbf{q})E(\mathbf{k})}\right]\times\frac{1-f\bigl[E(\mathbf{k}+\mathbf{q})\bigr]-f\bigl[E(\mathbf{k})\bigr]}{\omega-\bigl[E(\mathbf{k}+\mathbf{q})+E(\mathbf{k})\bigr]+\mathrm{i}\Gamma}+\sum_{\mathbf{k}}\frac{1}{4}\left[1-\frac{\xi(\mathbf{k}+\mathbf{q})\xi(\mathbf{k})+\Delta(\mathbf{k}+\mathbf{q})\Delta(\mathbf{k})}{E(\mathbf{k}+\mathbf{q})E(\mathbf{k})}\right]\times\frac{f\bigl[E(\mathbf{k}+\mathbf{q})\bigr]+f\bigl[E(\mathbf{k})\bigr]-1}{\omega+\bigl[E(\mathbf{k}+\mathbf{q})+E(\mathbf{k})\bigr]+\mathrm{i}\Gamma}\,. \tag{6.13}$$

Here the first term on the right-hand side allows for scattering of quasiparticles, and the second and third terms are responsible for the creation and annihilation of a pair of quasiparticles. In the case of creation (or annihilation), the minimum pair energy is Δ, with the result that the second and third terms can be ignored if $\omega \ll 2\Delta$. The first term has resonances at

$$\omega = E(\mathbf{k}+\mathbf{q}) - E(\mathbf{k})\,, \tag{6.14}$$

and these resonances are responsible for the peaks in $S(\mathbf{q},\omega)$.

If the symmetry of the order parameter allows for zeros for the gap, at low temperatures the quasiparticles concentrate near the corresponding values of $\mathbf{k}$. In the two-dimensional case the zeros appear on lines in $\mathbf{k}$-space. At the points of intersection of these lines and the Fermi surface the energy of excitations is zero. We denote these points by $\mathbf{k}_i$. Then we have the following equations:

$$E(\mathbf{k}_i)=0\,,\qquad \Delta(\mathbf{k}_i)=0\,,\qquad \mathbf{k}_i\in\mathbf{k}_\mathrm{F}\,. \tag{6.15}$$

At low temperatures, quasiparticle whose quasimomenta are close to $\mathbf{k}_i$ dominate in scattering processes. In the scattering of quasiparticles in the neighborhood of the same point $\mathbf{k}_i$, the scattering vector $\mathbf{q}$ is, obviously, small compared to $\mathbf{k}_\mathrm{F}$ for $\omega<\Delta<\varepsilon_\mathrm{F}$. However, quasiparticles can hop from the neighborhood of one point $\mathbf{k}_i$ to the neighborhood of another point $\mathbf{k}_j$, provided that condition (6.14) is met. In this case, as condition (6.14) implies, the scattering vector $\mathbf{q}$ is large. Thus, it becomes clear that resonances lead to peaks in the dynamic structure factor. The arrangement of these peaks is fully determined by the symmetry of the order parameter and the geometry of the Fermi surface. A peak at small values of $\mathbf{q}$ is masked by intense Bragg scattering, while the peaks at large values of $\mathbf{q}$, which emerge due to quasiparticle hopping between different zeros of the gap $\Delta(\mathbf{k})$ are observable (at least in principle). For a square lattice with a $\mathrm{d}_{x^2-y^2}$-wave order parameter, the arrangement of the expected peaks is determined by the vectors $(2k_\mathrm{F},2k_\mathrm{F})$, $(2k_\mathrm{F},0)$, and $(0,2k_\mathrm{F})$, when in the model that allows only for nearest-neighbor hopping k_F can be found from the equation for the chemical potential:

$$\cos k_\mathrm{F} = -\frac{\mu}{4t}\,.$$

Lu [120] calculated (6.13) for parameter values and a Fermi surface corresponding to the compound $La_2Sr_xCuO_4$. However, in the experimentally measured structure factor $S(\mathbf{q},\omega)$ considered a function of $\mathbf{q}$ (i.e. with ω fixed) no special peaks were found [117]. Zha et al. [121] calculated $\chi(\mathbf{q},\omega)$ by applying the RPA technique in the three-band model of the compound YBCO. Here, too, no peaks were discovered in $S(\mathbf{q},\omega)$. At the same time, the quantity $\mathrm{Im}\,\chi(\mathbf{q},\omega)$, measured via inelastic neutron scattering, was found to exhibit a temperature behavior at low frequencies that agreed with the assumption that the order parameter is $\mathrm{d}_{x^2-y^2}$-wave. For instance, near T_c a temperature maximum was found to exist for frequencies $\omega \leqslant 3$ meV, and this maximum disappeared at high frequencies, $\omega \approx 6$ meV, in accordance with the assumption that the order parameters is of the d-wave type. The absence of the predicted peaks in $S(\mathbf{q},\omega)$ in some experiments [117, 121] does not mean, however, that in the studied cuprates the gap $\Delta(\mathbf{k})$ has no zeros. These peaks could be masked by electron scattering by impurities if the samples are not clean enough. Notwithstanding the failure of the experiments conducted by Mason et al. [117] and Zha et al. [121], we must assume that neutron spectroscopy is one of the direct methods by which zeros in the superconducting order parameter of unconventional symmetry can be detected.

In conclusion of this section we would like to mention papers [122 – 127] which describe the latest achievements in the experimental study of the symmetry of the order parameter in cuprates.

7. The role of impurities

7.1 The gap, the superconducting transition temperature, and the density of states

For ordinary superconductors, the effect of impurities on the properties of the superconducting state was established long ago. Nonmagnetic impurities have a small effect on T_c (Anderson's theorem) — their role amounts to isotropization of the gap. On the contrary, magnetic impurities strongly suppress T_c (the Abrikosov – Gor'kov depairing mechanism) and lead to formation of a gapless state [128]. For superconductors with unusual order parameters, nonmagnetic impurities may have a strong effect on T_c and other properties. This problem was first studied theoretically for systems with heavy fermions [129] and recently for high-T_c compounds [130, 131]. It was found that, in superconductors with an anisotropic order parameter that has zeros at the Fermi surface, nonmagnetic impurities can strongly suppress T_c, and that the extent of this suppression depends on the symmetry of the order parameter, a fact that can be used to identify this symmetry by the behavior of many properties of superconductors considered as functions of the impurity concentration. On the other hand, magnetic impurities suppress T_c in the same way as they do in ordinary superconductors.

The marked difference between s- and d-wave superconductors in relation to impurities can be understood even in the weak-coupling setting. The matrix of the Green's function for a superconductor, $g(\mathbf{k},\omega_n)$, with a nonmagnetic impurity has a form as that for a pure superconductor,

$$g(\mathbf{k},\omega_n)=\frac{\tilde{\omega}\tau_0+\tilde{\xi}_k\tau_3+\tilde{\Delta}_k\tau_1}{\tilde{\omega}^2-\tilde{\xi}_k-|\Delta_k|^2}\,, \tag{7.1}$$

with the renormalized frequency $\tilde{\omega}=\omega-\Sigma_0$, quasiparticle energy $\tilde{\xi}_k=\xi_k-\Sigma_3$, and order parameter $\tilde{\Delta}_k=\Delta_k-\Sigma_1$. In the Born approximation for scattering, the quantities

$\Sigma_\alpha(\alpha = 0, 1, 3)$ are the corresponding elements of the matrix

$$\Sigma(\mathbf{k}, \omega_n) \equiv \sum_\alpha \Sigma_\alpha(\mathbf{k}, \omega) = \sum_{\mathbf{k}'} \mathcal{U}_{\mathbf{k}\mathbf{k}'} g(\mathbf{k}', \omega_n) . \tag{7.2}$$

Here $\mathcal{U}_{\mathbf{k}\mathbf{k}'}$ is the matrix element of the electron–impurity center interaction potential. For s-scattering, $\mathcal{U}_0$ is independent of the wave vectors $\mathbf{k}$ and $\mathbf{k}'$. Then Σ_α depends only on the frequency ω_n.

To find the superconducting transition temperature T_c, we can limit ourselves to the Δ-linear approximation. Then the matrix equation (7.2) splits into a pair of equations for $\tilde{\omega}$ and $\tilde{\Delta}$:

$$\tilde{\omega}_n = \omega_n + i\gamma_0 \int d\xi \int_0^{2\pi} \frac{d\theta}{2\pi} \frac{\tilde{\omega}_n}{\tilde{\omega}_n^2 + \xi^2} , \tag{7.3}$$

$$\tilde{\Delta}_n = \Delta_n + i\gamma_0 \int d\xi \int_0^{2\pi} \frac{d\theta}{2\pi} \frac{\tilde{\Delta}_n}{\tilde{\omega}_n^2 + \xi^2} \tag{7.4}$$

(we have ignored the renormalization of the quasiparticle spectrum $\xi_{\mathbf{k}}$). Here $\gamma_0 = n_i \pi N(0) \mathcal{U}_0$ is the isotropic scattering frequency, and n_i is the impurity concentration. Equation (7.3) yields the well-known formula for frequency renormalization,

$$\tilde{\omega}_n = \omega_n + \gamma_0 \operatorname{sign} \omega_n . \tag{7.5}$$

The linearized equation for the gap Δ_n, which is used to find T_c, has the form

$$\Delta_n(\mathbf{k}) = T_c \sum_{n'} \int \frac{d\mathbf{k}'}{(2\pi)^2} V_{\mathbf{k}\mathbf{k}'} \frac{\tilde{\Delta}_n(\mathbf{k}')}{\tilde{\omega}_{n'}^2 + \xi_{\mathbf{k}'}^2} , \tag{7.6}$$

with the wave vectors $\mathbf{k}$ and $\mathbf{k}'$ lying on the Fermi surface. Let us examine a two-dimensional system with an isotropic Fermi surface and a d-wave pairing potential:

$$V_{\mathbf{k}\mathbf{k}'} \equiv V(\theta, \theta') = V \psi_d(\theta) \psi_d(\theta') , \tag{7.7}$$

where $\psi_d(\theta) \sim \cos 2\theta$ for a $d_{x^2-y^2}$-wave state. Equation (7.4) shows that the impurity term vanishes after we have integrated with respect to θ, so that the gap function is not renormalized:

$$\tilde{\Delta}_n = \Delta_n . \tag{7.8}$$

For the anisotropic s-state

$$V(\theta, \theta') = V \left| \psi_s(\theta) \psi_s(\theta') \right| \tag{7.9}$$

with the same zeros at the Fermi surface as in the case of the $d_{x^2-y^2}$-state, Eqn (7.4) has the solution

$$\tilde{\Delta}_n = \Delta_n + \frac{2\sqrt{2}\,\gamma_0}{\pi |\omega_n|} \Delta_n^0 . \tag{7.10}$$

Equations (7.5)–(7.10) lead to an equation for T_c:

$$\ln \frac{T_{c0}}{T_c} = a \left[\psi\left(\frac{1}{2} + \frac{\gamma_0}{2\pi T_c} \right) - \psi\left(\frac{1}{2} \right) \right] , \tag{7.11}$$

where $a = 1$ for the $d_{x^2-y^2}$-symmetric case and $a = 1 - 8/\pi^2$ for anisotropic s-pairing [130, 131].

Thus, for $d_{x^2-y^2}$-wave superconductors the equations for T_c coincide with the equation of the Abrikosov–Gor'kov theory for ordinary superconductors with magnetic impurities [128]. This means that nonmagnetic impurities strongly suppress T_c in such superconductors. The critical concentration n_{c0} at which T_c vanishes can be found from the formula $\gamma = \gamma_c \approx 0.88 T_{c0}$. In the anisotropic s-case the dependence of T_c on γ is much weaker, so that for $\gamma \gg T_{c0}$ we have $T_c = T_{c0}\left[1 - a \ln(\gamma/\pi T_{c0})\right]$ (Fig. 19). Outside the scope of the Born approximation the effect of impurities on a superconductor with an anisotropic order parameter was studied by Borkowski and Hirschfeld [130] and Fehrenbacher and Norman [131], who used the T-matrix formalism [129]. Qualitatively, the results were the same. Even in the unitary limit (which is the opposite of the Born approximation), the dependence of T_c on the intensity of impurity scattering resembles the obtained in [130, 131]. Note that the role of anisotropic scattering by impurities (which, in addition to s-scattering, incorporates processes with finite orbital angular momentum) has been discussed by Posazhennikova and Sadovskii [133].

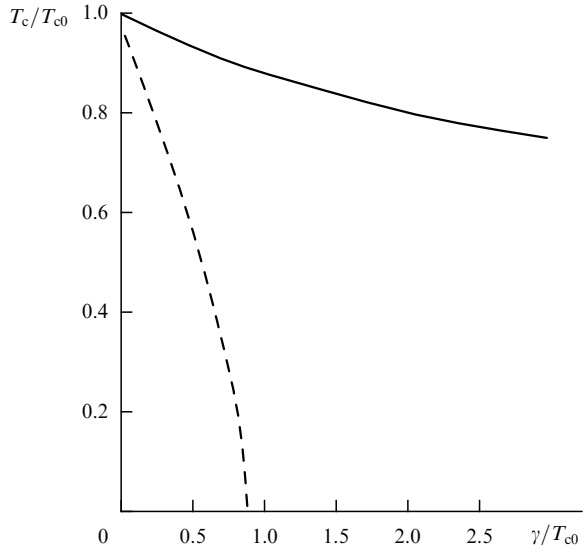

Figure 19. Superconducting transition temperature T_c as a function of the disorder parameter γ/T_{c0}, calculated in the Born approximation for a $d_{x^2-y^2}$-wave superconductor and an anisotropic s-wave superconductor [132].

The presence of nonmagnetic impurities in d-wave superconductors leads to another important effect, the emergence of a finite density of states at the Fermi level. The first to show this were Gor'kov and Kalugin [134], who studied superconductivity in systems with heavy fermions. Later the hypothesis was corroborated by Borkowski and Hirschfeld [130] and Fehrenbacher and Norman [131], who also calculated the frequency dependence of the spectral density of states $A(\mathbf{k}, \omega)$ for s- and d-wave superconductors with nonmagnetic impurities (Fig. 20). The interaction with the impurities was taken into account in the Born approximation. Figure 20 shows that impurities in an anisotropic s-wave superconductor (with zeros at the Fermi surface) open a gap whose width increases with the impurity concentration. The gap opens over the entire Fermi surface. At the same time, in d-wave superconductors the superconducting state remains gapless.

If the impurity has a localized magnetic moment, the exchange term $J(\mathbf{S}\boldsymbol{\sigma})$ leads to a depairing interaction, and the

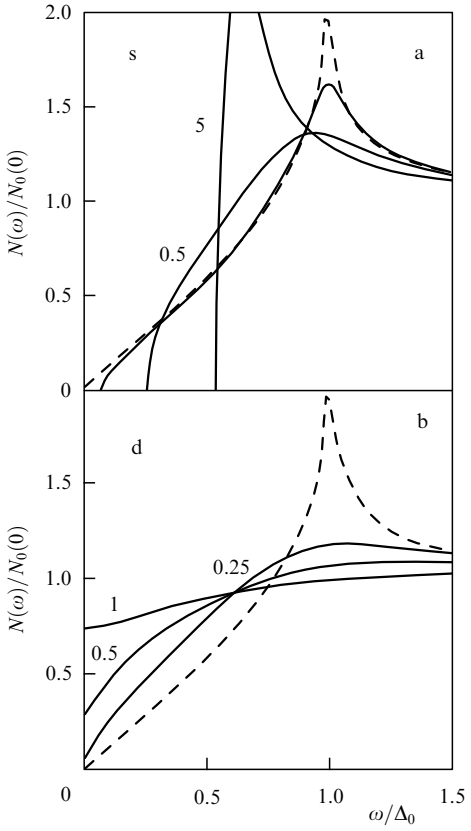

Figure 20. Normalized density of states for an s-wave superconductor (a) and a d-wave superconductor (b) for different values of the parameter γ_0/Δ_0. The dashed curves refer to a pure superconductor [130].

resulting effect of impurities is determined by the ratio of the magnetic impurity frequency $\gamma_s = n_i J^2 S(S+1)N(0)$ to the potential-scattering frequency γ_0 (Fig. 21). In all cases, the gap induced in s-wave superconductors increases in size with the potential-scattering intensity, but finally, thanks to the switch-on of the magnetic depairing interaction, the gap size passes its maximum and vanishes.

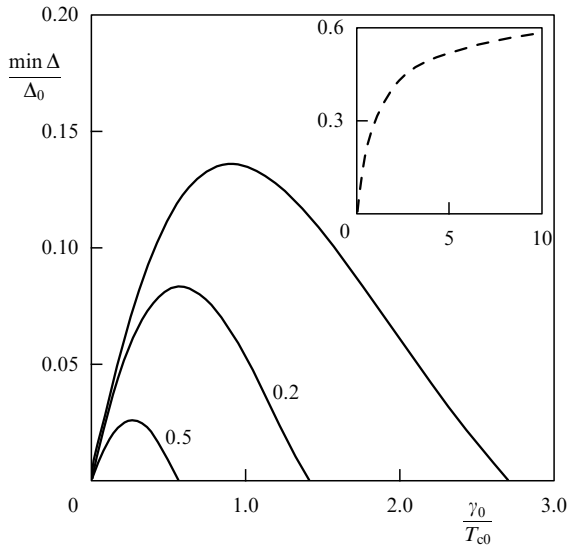

Figure 21. Relative value of an impurity gap induced in an anisotropic s-wave superconductor as a function of the impurity concentration in relation to the magnetic-to-impurity scattering ratio γ_s/γ_0. The dashed curve in the inset refers to the case of a nonmagnetic impurity [130].

The various approximations used in analytic calculations of the dependence of T_c on the impurity concentration and the parameters of scattering by impurities have been checked by Xiang and Wheatley [135], who solved the equation for the gap on a square lattice of 21×21 atoms with several impurity centers. The calculations were carried out under the assumption that $T = 0$ and with averaging over a large number of impurity configurations and with a large set of values of two scattering parameters, V_0 and V_1, where V_0 corresponds directly to scattering by an impurity center and V_1 to scattering by the neighbors nearest to that center. In this way not only isotropic scattering was included in the picture but so was scattering with finite orbital angular momentum. The solution for a gap function with an isolated impurity revealed deep minima in $\Delta(\mathbf{r})$ at points occupied by impurity centers, and the local density of states was found to oscillate. The finite impurity concentration averages these oscillations. If the concentration dependence of the gap function at $T = 0$ is assumed to be equivalent to the dependence of T_c, the results of numerical calculations are in good agreement with the analytic results obtained by the self-consistent T-matrix technique in both limits, one corresponding to the Born approximation and the other to the unitary limit for both s- and d-wave superconductors. In particular, for d-wave superconductors a finite density of states appears at the Fermi level, while a gap is induced for anisotropic s-wave superconductors with zeros at the Fermi surface. It was found that the effect of impurities depends on the degree of localization of the impurity potential: the weaker the localization the stronger the effect (see also Ref. [136]).

Note that Riera et al. [137] investigated the effect of impurities on the formation of Cooper pairs in the Tj-model using the technique of exact diagonalization of small clusters. The starting point of their studies was an earlier result obtained by the same technique: in the two-dimensional Tj-model on a square lattice (without impurities) for a half-filled band, a bound state of two holes appears for $J > J_c \sim 0.3t$ with a $d_{x^2-y^2}$-symmetric wave function of the pair. It was shown, by numerical calculations, that a nonmagnetic impurity has a stronger depairing effect on Cooper pairs than a magnetic impurity ($S = 1/2$). Therefore, this effect, described earlier in this review for the simple model of a superconductor, also manifests itself in strongly correlated electron models.

Nonmagnetic impurities have been found to suppress T_c in high-T_c compounds. For instance, it is known that a low concentration of Zn atoms substituting Cu (2%) in YBCO reduces T_c by 25%. It is difficult to compare this result with theoretical estimates because of the unknown scattering parameters (e.g. the fact that potential scattering dominates is ignored). There are certain arguments in favor of the fact that Zn atoms change the magnetic correlations in their vicinity and lead to additional scattering by an impurity center accompanied by spin flip [138]. In this case, the magnetic impurity center effectively behaves as a magnetic impurity center. The problem merits additional investigations.

7.2 Thermodynamics and kinetics

The differences in the dependence of T_c on impurity concentration for anisotropic superconductors of the d- and s-wave types can be studied (at least in principle) with the aim

of identifying the symmetry of the order parameter. However, the other properties of superconductors, properties that are sensitive to the presence of impurities, are more specific. Among these properties are the penetration depth λ, the upper critical field H_{c2}, IR absorption, and Raman spectroscopy.

In Section 6 we showed that in pure d-wave superconductors at temperatures much lower than T_c, the deviation $\Delta\lambda$ of the penetration depth for its value at $T = 0$ is, due to the zeros of the gap at the Fermi surface, proportional to T. However, experiments on high-T_c single crystals revealed that $\Delta\lambda \sim T^2$. Hardy et al. [70] hypothesized that the change in the temperature dependence of the penetration depth is due to the presence of impurities. A theoretical investigation of this problem was done by Hirschfeld and Goldenfeld [139]. Calculating the penetration depth requires knowing the electromagnetic response tensor K, which links the current $\mathbf{j}$ to the vector potential $\mathbf{A}$: $\mathbf{j} = K\mathbf{A}$. The penetration depth is determined by the eigenvalues of this tensor. If $K_{\alpha\beta}$ is diagonal, λ_α can be found from the relationship $\lambda_\alpha^{-2} = (4\pi/c)K_{\alpha\alpha}$. In the BCS model, the tensor $K_{\alpha\beta}$ is determined by the formula

$$K_{\alpha\beta} = \frac{e^2}{c}\left\langle v_\alpha(\mathbf{k})v_\beta(\mathbf{k})\int_0^\infty \mathrm{d}\omega \,\mathrm{th}\,\frac{\omega}{2T}\,\mathrm{Re}\,\frac{\Delta_\mathbf{k}^2}{(\tilde{\omega}^2-\Delta_\mathbf{k}^2)^{3/2}}\right\rangle, \quad (7.12)$$

where $v_\alpha(\mathbf{k})$ is the velocity at the Fermi surface, and $\langle\ldots\rangle$ stands for averaging over the Fermi surface. The quantity $\tilde{\omega}$ is the renormalized (due to the impurity) frequency: $\tilde{\omega} = \omega - \Sigma_0(\omega)$. The calculation of $\Sigma_0(\omega)$ by the self-consistent T-matrix technique makes it possible, via Eqn (7.12), to find $\lambda(T)$ for different impurity scattering intensities. In the event of resonance scattering, which corresponds to the parameter interval between the Born and unitary limits, Hirschfeld and Goldenfeld [139] found that for d-wave superconductors there is crossover between linear and quadratic behavior of $\Delta\lambda$ with a crossover temperature $T^* \sim \sqrt{n_i}$ (in the case of resonance scattering this is true to within logarithmic corrections). It occurs that $\Delta\lambda \sim T$ for $T < T^* \ll T_c$ and $\Delta\lambda \sim T^2$ for $T^* < T \ll T_c$. These results agree with the results of measurements involving the YBCO system [70].

The difference between s- and d-wave superconductors manifests itself in the behavior of the slope of the temperature dependence of H_{c2} with respect to the impurity concentration [133]. The upper critical field can be expressed in terms of the correlation length:

$$H_{c2} = \frac{\Phi_0}{2\pi\xi(T)^2} \quad (7.13)$$

(Φ_0 is the quantum of magnetic flux, and $\xi(T)$ can be found from the Ginzburg–Landau expansion for the free energy in the BCS model). For a $\mathrm{d}_{x^2-y^2}$-wave order parameter, $\mathrm{d}H_{c2}/\mathrm{d}T$ rapidly decreases with increasing impurity concentration on a scale $\gamma_0 \sim T_{c0}$, while for an anisotropic s-wave superconductor, $\mathrm{d}H_{c2}/\mathrm{d}T$ increases with γ_0. When $\gamma_0 \gg T_{c0}$, the slope is determined by the Gor'kov formula [140]:

$$\frac{\sigma}{N(0)}\left|\frac{\mathrm{d}H_{c2}}{\mathrm{d}T}\right|_{T_c} = \frac{8e^2}{\pi^2}\,H_{c2}\,, \quad (7.14)$$

which was obtained for an ordinary isotropic superconductor in the 'dirty' limit. Here $\sigma = N(0)e^2v_F/3\gamma_0$ is the electron conductivity in the normal phase. Thus, in an anisotropic s-wave superconductor, the slope of H_{c2} also varies monotonically with γ_0 when γ_0 is large.

IR absorption, which is described by the conductivity's real part, exhibits specific properties in the case of anisotropic superconductors with zeros of the gap at the Fermi surface [141–144]. The frequency dependence $\sigma(\omega)$ in this case is extremely sensitive to the presence of impurities. Generally, this dependence is determined by the inelastic scattering of electrons by Bose excitations of the system and by elastic impurity scattering. In the BCS model the conductivity is calculated by the formula

$$\mathrm{Re}\,\sigma_{\alpha\beta}(\omega) = -\frac{\mathrm{Im}\,\Lambda_{\alpha\beta}(\omega)}{\omega}\,, \quad (7.15)$$

where

$$\mathrm{Im}\,\Lambda_{\alpha\beta}(\omega) = \pi e^2\int \mathrm{d}\omega'\left\langle v_\alpha(\mathbf{k})v_\beta(\mathbf{k})\left[f(\omega+\omega') - f(\omega')\right]\mathrm{Tr}\left[A(\mathbf{k},\omega+\omega')A(\mathbf{k},\omega')\right]\right\rangle, \quad (7.16)$$

and $A(\mathbf{k},\omega) = -(1/\pi)\,\mathrm{Im}\,G(\mathbf{k},\omega)$ is the spectral density of the matrix one-particle Green's function. Hirschfeld et al. [144] used the Hubbard model on a square lattice with an electron spectrum

$$\varepsilon(\mathbf{k}) = -2t(\cos k_x + \cos k_y)\,.$$

They allowed for scattering by spin fluctuations in the electron self-energy $\Sigma(\mathbf{k},\omega)$, and the spin susceptibility was accounted for in the RPA. The results of numerical calculations by Eqns (7.15) and (7.16) for systems with a nonmagnetic impurity characterized by the scattering parameter Γ are depicted in Fig. 22 together with the experimental data of Basov et al. [146] on the YBCO crystal. Clearly, there is

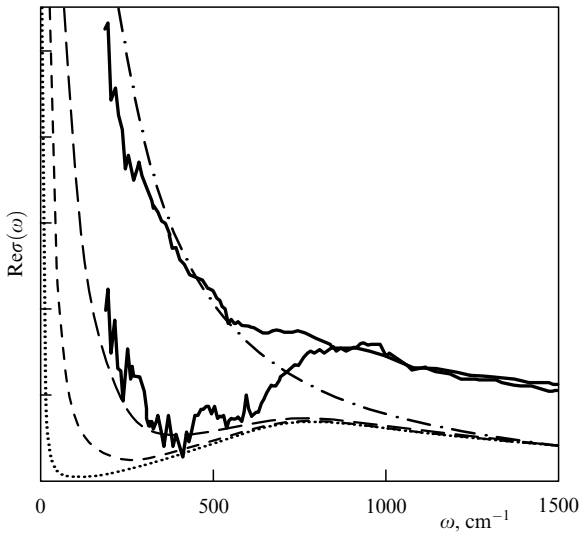

Figure 22. Real part of the microwave conductivity calculated for the normal phase with $T = T_c$ and $\Gamma = 0.018T_c$ (the dot-dash curve) and the superconducting phase with $T = 0.1T_c$ [145] as compared to the experimental data (the solid curve) on conductivity along the **a** axis in the normal ($T = 100$ K) and superconducting ($T = 20$ K) phases of YBCO crystal [146]. The dashed and dotted curves represent the results of calculations for the superconducting phase with the following parameters of impurity scattering: $\Gamma = 0.018T_c$ (long-dash curve), $\Gamma = 0.1T_c$ (short-dash curve), and $\Gamma = 0.008T_c$ (dotted curve).

qualitative agreement between the theoretical and experimental results, which is an indication that the order parameter has zeros on the Fermi surface due to the spin-fluctuation pairing mechanism.

7.3 Localization

It is well known that when the disorder in a metallic system is substantial, Anderson localization of the charge carrier can emerge in the system [147]. The essence of such localization is that in the continuous spectrum a point ω_c emerges (the mobility edge) above which all the states are delocalized (extended) but below which these states are localized, i.e. their wave functions decrease exponentially with increasing distance, with the extent of localization specified by a parameter known as the localization length, R_c. The disorder created by impurities can lead to the localization of the low-energy states in an ordinary superconductor, too [148, 149]. When we are dealing with d-wave superconductors, the problem of localization is much more complicated. Earlier we saw that because of zeros in the superconducting order parameter the presence of impurities in such superconductors leads to a finite density of states at the Fermi surface, while in pure d-wave superconductors $N(\omega) \sim \omega$ when $\omega \ll \Delta_0$. What is the nature of the low-energy states in such a superconductor in which there are nonmagnetic impurities of a certain concentration? The answer to this question is especially important if we wish to interpret the results of experiments involving high-T_c compounds, since such compounds always have impurities and, on the other hand, many thermodynamic and transport properties of superconductors are determined by the contribution of low-energy states.

Using the idea of scaling, Lee [150] demonstrated that impurities in d-wave superconductors in the unitary limit generate localized states below the mobility edge ω_c, whose value is a fraction of the maximum gap Δ_0. The mobility edge and the localization length depend on Δ_0 in the following manner:

$$\omega_c \sim \Delta_0^{1/2}; \qquad R_c \sim \Delta_0^{-1/2} \exp\left(\frac{\varepsilon_F}{\Delta}\right). \tag{7.17}$$

Balatsky and Salkola [151] criticised Lee's work on the grounds that it does not allow for electron hopping from one impurity center to another due to the long-range tails of the single-impurity states. This hopping plays an important role in the localization of electronic states. The tails emerge because of the zeros in the superconducting order parameter, and their contribution may be lost in coarse averaging over the impurity configurations. Balatsky and Salkola [151] believe that in the case of d-wave superconductors one must begin with the exact solution of the single-impurity. The wave function at point $r = 0$ of the impurity state varies in space according to the law [152]

$$\psi_{imp}(r,\theta) \sim \sin(k_F r) \begin{cases} \dfrac{1}{\sqrt{r}} \exp\left[-\dfrac{r}{\xi(\theta)}\right], & \theta \not\approx \dfrac{\pi}{4} + n\dfrac{\pi}{2}, \\ \dfrac{1}{r}, & \theta \approx \dfrac{\pi}{4} + n\dfrac{\pi}{2}, \end{cases} \tag{7.18}$$

where $\xi(\theta) \equiv \hbar v_F/|\Delta(\theta)| = \xi_0/|\cos 2\theta|$ is the angle between the radius vector $\mathbf{r}$ and the crystallographic axis in the base plane, and $n = 0, 1, 2, 3$ correspond to four diagonals of the square on which the zeros of the order parameters are arranged. It is along these directions that the wave function has long-range tails. If another impurity atom lands on one of these diagonals, there is an impurity – impurity interaction even if the distance is great. Since the energies of the states centered at these two impurities are the same, the interaction is resonant, i.e. the states will be hybridized. Thus, if the impurity concentration is finite, the impurity states become collectivized via the long-range tails. This conclusion is in sharp contrast with the results of weak-localization theory, which predicts that all quasiparticles in a two-dimensional system are localized.

When the impurity concentration is low, or $\xi^2 n_i \ll 1$, the matrix element of electron hopping between two impurities centered at $\mathbf{r}_i$ and $\mathbf{r}_j$ is given by the formula $V_{ij} = G_0(\mathbf{r}_i - \mathbf{r}_j, 0)$, where $G_0(\mathbf{r}, \omega)$ is the matrix Green's function for a pure superconductor. In these conditions, a superconductor with impurities is described by the effective Hamiltonian

$$H = \sum_{ij} \psi_i^\dagger V_{ij} \psi_j + \sum_i \psi_i^\dagger \varepsilon_i \tau_3 \psi_i, \tag{7.19}$$

where ψ_i is the wave function in the Nambu representation, and the ε_i are the impurity levels. It is assumed that these levels are distributed at random within a certain energy interval $0 \leqslant \varepsilon_i \leqslant W$ with an equal probability $1/W$. The matrix element of overlap along the diagonals varies with distance as $1/r_{ij}$:

$$V_{ij} \sim -V_0 \frac{\hbar v_F}{r_{ij}} \sin(k_F r_{ij}) \tau_3, \tag{7.20}$$

where V_0 is a dimensionless parameter characterizing the magnitude of the matrix element. Analysis of model (7.20) shows that the quasiparticle states induced by the impurities are delocalized states at energies $\omega < \omega_c$, where $\omega_c \sim \exp(-c/n_i)$ is the characteristic energy, which exponentially depends on the impurity concentration, and c is a positive constant. When $\omega > \omega_c$, the impurities form a band of localized states, with the result that there is the inversion of localized and delocalized states with respect to the mobility edge.

In view of the contradictory results achieved by two similar approaches to the problem of localization in a d-wave superconductor, the approach developed by Lee [150] and that developed by Balatsky and Salkola [151], Franz et al. [153] made numerical calculations for clusters of a square lattice containing up to 50×50 atoms and nonmagnetic impurities. The model included the Coulomb interaction V_0 at a single site and the attraction V_1 at neighbors, and all this leads to a d-wave superconductor. They used the mean-field approximation to write the equations for the superconductor with impurities in the site representation and solved these equations numerically by many iterations.

Since the impurity potential was specified only at a single site, the method made it possible to obtain the exact solution of the problem of an impurity in the normal phase. Numerical solution of the problem with one impurity center revealed that there is strong local suppression of the superconducting order parameter near the impurity. In solving the problem of several impurity atoms corresponding to a given impurity concentration, Franz et al. [153] allowed, in a self-consistent manner, for the effect of local suppression of the order

parameter. This effect proved to play an important role in the localization problem. Analysis of the solutions has shown that low-energy excitations are localized up to energies $\omega \approx t$. The mobility edge obtained in this way was found to be close to Lee's result of $\omega_c \approx 0.84t$, which was found for the same values of the parameters. Franz et al. [153] believe that the discrepancy between Lee's result and that of Balatsky and Salkola [151] stems from the fact that in similar calculations Balatsky and Salkola [151] ignored the local suppression of the d-wave order parameter. Self-consistent allowance for this effect leads to the conclusion that low-energy states in a d-wave superconductor are localized. New research on this subject is described in [154–190].

8. Summary

Can we state with all certainty that the spin-fluctuation mechanism of superconductivity dominates in the high-T_c superconductors of the copper-oxide group and that the superconducting order parameter is $d_{x^2-y^2}$-symmetric? While the second part of this main question can be resolved exclusively by experiments, the problem of the dominant pairing mechanism is in many respects a problem of theoretical concepts. The experimental data on the properties of the superconducting state in cuprates irrevocably indicate that an anisotropic order parameter with zero values of the gap at the Fermi surface is realized in such substances. Superconductors belonging to the lanthanum, yttrium–barium, and bismuth groups have been studied most thoroughly. The overwhelming majority of the results obtained as a result of low-temperature measurements of NMR parameters and the penetration depth, ARPES measurements, and many variants of interference measurements involving Josephson junctions suggest that the order parameter of these superconductors is $d_{x^2-y^2}$-symmetric. However, in some experiments on superconductors of the yttrium–barium group the d-symmetry could not be distinguished from the s^*-symmetry, which means that new methods and new classes of high-T_c superconducting compounds are needed for further experimental studies of the symmetry of the order parameter. This path of research is fraught with surprises. For instance, experiments on the temperature dependence of the penetration depth in electron-doped superconductors of the neodymium group suggest that the order parameter is more likely to be of s-wave type.

The spin-fluctuation mechanism of superconductivity indirectly supports the idea that the order parameter is of $d_{x^2-y^2}$-wave type. The relationship between these two features is established both in the phenomenological approach and in the microscopic approaches based on the Hubbard model and the tJ-model. Eliashberg-type equations for the effective electron–magnon interaction lie at the base of these approaches, which use the concept of spin-fluctuation pairing. It has been found that the renormalization of the quasiparticle spectrum caused by this interaction plays an important role in these approaches: renormalization leads to certain anomalies in the properties of the normal state of doped high-T_c superconducting compounds (e.g. their behavior differs from that of an ordinary Fermi liquid). Numerical calculations using the phenomenological and microscopic approaches have demonstrated the need to integrate over the entire $\mathbf{k}$-space in the Eliashberg equations instead of limiting oneself to a thin layer near the Fermi surface (as is done in the standard electron–phonon model of superconductivity). The reason is that the magnetic susceptibility near an antiferromagnetic transition (this susceptibility determines the effective electron–electron coupling) has a peak near the wave vector (π, π) and slowly diminishes as we move away from this point. We can obtain a high T_c of order 100 K only if we take into account the effective interaction over the entire $\mathbf{k}$-space, and it is remarkable that the solutions for a gap under these conditions are exactly $d_{x^2-y^2}$-symmetric. This explains why observations of such a case in experiments would be a strong argument in favor of the spin-fluctuation mechanism in high-T_c superconducting compounds.

Notwithstanding this important fact, the problem of the mechanism of high-T_c superconductivity in cuprates is far from being resolved. What is needed is a consistent microscopic theory for values of the model parameters corresponding to cuprates. If we take the one-band Hubbard model with two parameters, tz and U, the approaches discussed in Sections 3 and 4 deal with two limits, of weak and strong Coulomb interactions, while for cuprates the intermediate case of $U \gtrsim zt$ is more likely to be true. Thus, the main theoretical problem reduces to calculating the dynamic magnetic susceptibility near the half-filled band under the condition that $U \sim zt$. It is extremely difficult to find analytic algorithms for this intermediate case. In the case of a strongly correlated system ($U \gg zt$) we can use the tJ-model, but even this model does not provide an analytic method for calculating the magnetic susceptibility if the spin polaron model is inapplicable, i.e. if we are far from an antiferromagnetic state. And even if the magnetic susceptibility for $U \gtrsim zt$ were calculated, we still have to solve the difficult problem of renormalizing the vertex of the electron–magnon interaction in Eqn (1.3), which leads to Eliashberg equations.

We conclude that although a rigorous theory of the spin-fluctuation mechanism of high-T_c superconductivity in cuprates has yet to be developed, the experimental studies of the symmetry of the superconducting order parameter have provided the necessary basis for such a theory. At the same, some experimental facts seem to contradict the spin-fluctuation mechanism. What we mean is that the spin-fluctuation spectrum of the lanthanum and yttrium–barium systems lacks low-energy fluctuations, which are needed if we want an effective spin-fluctuation pairing mechanism to be realized. This fact is corroborated by the experimental data on inelastic neutron scattering; the interested reader can find a discussion of these data in Plakida's book [36]. Here we would only like to mention the latest experiments on $La_{2-x}Sr_xCuO_4$ single crystals with optimum Sr doping [180] and on $YBa_2Cu_3O_{6.6}$ [181]. In these two papers the reader can also find references to the different papers on this topic. The observed cutoff of the low-frequency part of the spin-fluctuation spectrum is often referred to as the magnetic-gap problem, although such terminology may distort the origin of this phenomenon. As shown by various theoretical investigations, the cutoff of the low-frequency branch of the spin susceptibility in the Hubbard model [29] and in the tJ-model [36] is the result of nesting in the electron spectrum at the wave vector $\mathbf{Q} = (\pi, \pi)$, which probably is a characteristic feature of an antiferromagnetic Fermi liquid. Thus, the suppression of the low-frequency part of the spectrum in cuprates may not be an argument against the spin-fluctuation pairing mechanism.

It must be said, however, that not all researchers believe in the concept of the spin fluctuation mechanism of pairing in cuprates. Some propose using the mechanism of pairing via

charge fluctuation. The reason stems from the fact that cuprates are highly polarizable substances. The most recent work in this field is that of Enz [162], where other papers on the subject are cited. Bulut and Scalapino [163] discuss the conditions under which the electron – phonon interaction can lead to superconductivity with a d-symmetric order parameter. The concept of a nearly antiferromagnetic Fermi liquid and the spin-fluctuation mechanism of superconductivity is criticised in the recent works of Anderson [188 – 190]. There he proposed an alternative mechanism of superconductivity in cuprates based on the idea of electron confinement in the Cu – O planes, with the interplanar electron transition being the reason for a coherent superconducting order parameter in these systems. A discussion of this mechanism, however, lies outside the scope of the present review.

In conclusion we would like to mention the work of Mathur et al. [191], who used the spin-fluctuation mechanism to explain superconductivity in a number of cerium-based compounds belonging to heavy fermions. They found that, for the compounds $CePd_2Si_2$ and $CeIn_3$, the situation resembles that with cuprates. In normal conditions these compounds are antiferromagnets with wave vectors [110] and [111], respectively, and have a Neel temperature of 10 K. Under pressure, T_N drops rapidly and at a pressure P of about 20 kbar the antiferromagnetic order disappears. At the same time, in a narrow region in the vicinity of this critical value of pressure a superconducting state emerges with $T_c < 1$ K. For $T > T_c$ the properties of the normal phase differ from ordinary Fermi-liquid behavior. For instance, within a broad temperature interval the electrical resistance varies with temperature according to a power law with an exponent $1.2 < n < 1.5$. The phase diagrams for these compounds in the (T, P) plane are similar to those for cuprates in the (T, n) plane. Such similarity led Mathur et al. [191] to believe that the spin-fluctuation mechanism of electron pairing operates in these cerium compounds. It would be interesting to establish the symmetry of the superconducting order parameter for these compounds.

References

1. Izyumov Yu A *Usp. Fiz. Nauk* **167** 465 (1997) [*Phys. Usp.* **40** 445 (1997)]
2. Ovchinnikov S G *Usp. Fiz. Nauk* **167** 1043 (1997) [*Phys. Usp.* **40** 993 (1997)]
3. Izyumov Yu A *Usp. Fiz. Nauk* **165** 403 (1995) [*Phys. Usp.* **38** 385 (1995)]
4. Berk N F, Schrieffer J R *Phys. Rev. Lett.* **17** 433 (1966)
5. Eliashberg G M *Zh. Eksp. Teor. Fiz.* **38** 966 (1960) [*Sov. Phys. JETP* **11** 696 (1960)]; **39** 1437 (1960) [**12** 1000 (1961)]
6. Scalapino D J, Loh E (Jr), Hirsch J E *Phys. Rev. B* **35** 6694 (1987)
7. Bickers N E, Scalettar R T, Scalapino D J *Int. J. Mod. Phys. B* **1** 687 (1987)
8. Moriya T, Takahashi Y, Ueda K *J. Phys. Soc. Jpn.* **52** 2905 (1990)
9. Ueda K, Moriya T, Takahashi Y in *Electronic Properties and Mechanisms of High-T_c Superconductors* (Eds T Oguchi, K Kadowaki, T Sasaki) (Amsterdam: North-Holland, 1992)
10. Volovik G E, Gor'kov L P *Zh. Eksp. Teor. Fiz.* **88** 1412 (1985) [*Sov. Phys. JETP* **61** 843 (1985)]
11. Sigrist M, Rice T M *Z. Phys. B* **68** 9 (1987)
12. Pines D *Tr. J. Phys.* **20** 535 (1996)
13. Monthoux P, Balatsky A V, Pines D *Phys. Rev. Lett.* **67** 3448 (1991)
14. Monthoux P, Balatsky A V, Pines D *Phys. Rev. B* **46** 14803 (1992)
15. Monthoux P, Pines D *Phys. Rev. Lett.* **69** 961 (1992)
16. Monthoux P, Pines D *Phys. Rev. B* **47** 6069 (1993)
17. Monthoux P, Pines D *Phys. Rev. B* **49** 4261 (1994)
18. Millis A J, Monien H, Pines D *Phys. Rev. B* **42** 167 (1990)
19. Vidberg H J, Serene J W *J. Low Temp. Phys.* **29** 177 (1977)
20. Kampf A, Schrieffer J R *Phys. Rev. B* **41** 6399 (1990); **42** 7967 (1990)
21. Lenck St, Carbotte J P *Phys. Rev. B* **49** 4176 (1994)
22. Tifrea I, Crisan M, Grosu I *Phys. Rev. B* **55** 5998 (1997)
23. Lenck St, Carbotte J P, Dynes R C *Phys. Rev. B* **50** 10149 (1994)
24. Monthoux P, Scalapino D J *Phys. Rev. Lett.* **72** 1874 (1994)
25. Pao C-H, Bickers N E *Phys. Rev. Lett.* **72** 1870 (1994)
26. Bickers N E, Scalapino D J, White S R *Phys. Rev. Lett.* **62** 961 (1989)
27. Bickers N E, White S R *Phys. Rev. B* **43** 8044 (1991)
28. Tewordt L *J. Low Temp. Phys.* **15** 344 (1979)
29. Wermbter S, Tewordt L *Phys. Rev. B* **44** 9524 (1991)
30. Lenck St, Wermbter S, Tewordt L *J. Low Temp. Phys.* **80** 269 (1990)
31. Anderson P W *Science* **235** 1196 (1987)
32. Kane C L, Lee P A, Read N *Phys. Rev. B* **39** 6880 (1989)
33. Plakida N M et al. *Phys. Rev. B* **55** R11997 (1997)
34. Belinicher V I et al. *Phys. Rev. B* **51** 6076 (1995)
35. Ohta Y et al. *Phys. Rev. Lett.* **73** 324 (1994)
36. Plakida N M *Vysokotemperaturnye Sverkhprovodniki* [High-Temperature Superconductors] (Moscow: Mezhdunarodnaya Programma Obrazovaniya, 1996) [Translated into English: *High-Temperature Superconductivity* (Berlin: Springer, 1995)]
37. Xu J-H, Ren Y, Ting C S *Phys. Rev. B* **52** 7663 (1995)
38. Soininen P I, Kallin C, Berlinsky A J *Phys. Rev. B* **50** 13883 (1994)
39. Berlinsky A J et al. *Phys. Rev. Lett.* **75** 2200 (1995)
40. Franz M et al. *Phys. Rev. B* **53** 5795 (1995)
41. Volovik G E *Pis'ma Zh. Eksp. Teor. Fiz.* **58** 457 (1993) [*JETP Lett.* **58** 469 (1993)]
42. Walker M B, Timusk T *Phys. Rev. B* **52** 97 (1995)
43. Ichioka M et al. *Phys. Rev. B* **53** 2233 (1996)
44. Schopohl N, Maki K *Phys. Rev. B* **52** 490 (1995)
45. Maki K, Schopohl N, Won H *Physica B* **204** 214 (1995)
46. Heeb R et al. *Phys. Rev. B* **54** 9385 (1996)
47. Sun A G et al. *Phys. Rev. Lett.* **72** 2267 (1994)
48. Arovas D P et al. *Phys. Rev. Lett.* **79** 2871 (1997)
49. Zhang S C *Science* **275** 1089 (1997); Burgess C P, Lütken C A *Phys. Rev. B* **57** 8642 (1998); Burgess C P et al. *Phys. Rev. B* **57** 8549 (1998)
50. Walker M B, Pairor P, Zhitomirsky M E *Phys. Rev. B* **56** 9015 (1997)
51. Feder D L, Kallin C *Phys. Rev. B* **55** 559 (1997)
52. Micnas R, Ranninger J *Rev. Mod. Phys.* **62** 113 (1990)
53. Dagotto E, Nazarenko A, Moreo A *Phys. Rev. Lett.* **74** 310 (1995)
54. Nazarenko A et al. *Phys. Rev. B* **54** R768 (1996)
55. Keimer B *J. Appl. Phys.* **76** 6788 (1994)
56. Maggio-Aprile I et al. *Phys. Rev. Lett.* **75** 2754 (1995)
57. Liu M, Xing D Y, Wang Z D *Phys. Rev. B* **55** 3181 (1997)
58. Ruckenstein A E, Hirschfeld P J, Appel J *Phys. Rev. B* **36** 857 (1987)
59. Kotliar G *Phys. Rev. B* **37** 3664 (1988)
60. Donovan C O, Carbotte J P *Physica C* **252** 87 (1995)
61. Ren Y, Xu J-H, Ting C S *Phys. Rev. B* **53** 2249 (1996)
62. Musaelian K A et al. *Phys. Rev. B* **53** 3598 (1996)
63. Maki K, Beal-Monod M T *Phys. Rev. B* **55** 11730 (1997)
64. Zhang K et al. *Phys. Rev. Lett.* **73** 2484 (1994)
65. Wang Q, Wang Z D *Phys. Rev. B* **54** R15645 (1996)
66. Vicente Alvarez J J, Dominguez D, Balseiro C A *Phys. Rev. Lett.* **79** 1373 (1997)
67. Kopnin N B, Volovik G E *Phys. Rev. Lett.* **79** 1377 (1997)
68. Won H, Maki K *Europhys. Lett.* **30** 421 (1995)
69. Scalapino D J *Phys. Rep.* **250** 329 (1995)
70. Hardy W N et al. *Phys. Rev. Lett.* **70** 3999 (1993)
71. Bulut N, Scalapino D J *Phys. Rev. Lett.* **68** 706 (1992)
72. Bulut N, Scalapino D J *Phys. Rev. B* **45** 2371 (1992)
73. Hammel P C et al. *Phys. Rev. Lett.* **63** 1992 (1989)
74. Takanaka K, Kuboya K *Phys. Rev. Lett.* **75** 323 (1995)
75. Hanaguri T et al. *Physica B* **165&166** 1449 (1990)
76. Chen X K et al. *Phys. Rev. Lett.* **73** 3290 (1994)
77. Koike Y et al. *Phys. Rev. B* **54** R776 (1996)
78. Akhiezer A I, Pomeranchuk I Ya *Zh. Eksp. Teor. Fiz.* **36** 859 (1959) [*Sov. Phys. JETP* **9** 605 (1959)]
79. Wollman D A et al. *Phys. Rev. Lett.* **74** 797 (1995)
80. Wollman D A et al. *Phys. Rev. Lett.* **71** 2134 (1993)
81. Brawner D A, Ott H R *Phys. Rev. B* **53** 8249 (1996)
82. Chaudhari P, Lin S-Y *Phys. Rev. Lett.* **72** 1084 (1994)
83. Sun A G et al. *Phys. Rev. Lett.* **72** 2267 (1994)
84. Kleiner R et al. *Phys. Rev. Lett.* **76** 2161 (1996)
85. Kouznetsov K A et al. *Phys. Rev. Lett.* **79** 3050 (1997)

86. Kirtley J R, Moler K A, Scalapino D J *Phys. Rev. B* **56** 886 (1997)
87. Miller J H et al. *Phys. Rev. Lett.* **74** 2347 (1995)
88. Mathai A et al. *Phys. Rev. Lett.* **74** 4523 (1995)
89. Tanaka Y, Kashiwaya S *Phys. Rev. B* **56** 892 (1997)
90. lshimaru Y et al. *Phys. Rev. B* **55** 11851 (1997)
91. Sigrist M, Rice T M *J. Phys. Soc. Jpn.* **61** 4283 (1992)
92. Tsuei C C et al. *Phys. Rev. Lett.* **73** 593 (1994)
93. Tsuei C C *Science* **271** 329 (1996)
94. Kirtley J R et al. *Tr. J. Phys.* **20** 576 (1996)
95. Samanta M P, Datta S *Phys. Rev. B* **55** R8689 (1997)
96. Shen Z-X et al. *Phys. Rev. Lett.* **70** 1553 (1993)
97. Kelley R J et al. *Phys. Rev. B* **50** 590 (1994)
98. Ding H, Campuzano J C, Jennings G *Phys. Rev. Lett.* **74** 2784 (1995)
99. Ma J et al. *Science* **267** 862 (1995)
100. Ding H et al. *Phys. Rev. B* **54** R9678 (1996)
101. Ding H et al. *Phys. Rev. Lett.* **76** 1533 (1996)
102. Klein M V, Dierker S B *Phys. Rev. B* **29** 4976 (1984)
103. Devereaux T P et al. *Phys. Rev. Lett.* **72** 396 (1994)
104. Krantz M C, Cardona M *Phys. Rev. Lett.* **72** 3290 (1994)
105. Devereaux T P et al. *Phys. Rev. Lett.* **72** 3291 (1994)
106. Chen X K et al. *Phys. Rev. B* **48** 10530 (1993)
107. Wenger F, Kall M *Phys. Rev. B* **55** 97 (1997)
108. Morr D K, Chubukov A V *Phys. Rev. B* **56** 9134 (1997)
109. Manske D et al. *Phys. Rev. B* **56** 2940 (1997)
110. Marshall D S et al. *Phys. Rev. Lett.* **76** 4841 (1996)
111. Loeser A G *Science* **273** 325 (1996)
112. Ding H et al. *Nature* (London) **382** 51 (1996)
113. Ding H et al. *Phys. Rev. Lett.* **78** 2628 (1997)
114. Chen X K et al. *Phys. Rev. B* **56** R513 (1997)
115. Kivelson S, Emery V *Nature* (London) **374** 434 (1995)
116. Wen X-G, Lee P A *Phys. Rev. Lett.* **76** 503 (1996)
117. Mason T E et al. *Phys. Rev. Lett.* **71** 919 (1993)
118. Yamada K et al. *Phys. Rev. Lett.* **75** 1626 (1995)
119. Rossat-Mignot J et al., in *Frontiers in Solid State Science* (Singapore: World Scientific, 1993) p. 265
120. Lu J P *Phys. Rev. Lett.* **68** 125 (1992)
121. Zha Y, Levin K, Si Q *Phys. Rev. B* **47** 9124 (1993)
122. Carbotte J P et al. *Phys. Rev. B* **51** 11798 (1995)
123. Jiang C et al. *Phys. Rev. B* **54** 1264 (1996)
124. Zhitomirsky M E, Walker M B *Phys. Rev. Lett.* **79** 1734 (1997)
125. Williams G V M et al. *Phys. Rev. Lett.* **78** 721 (1997)
126. Panagopoulos C et al. *Phys. Rev. Lett.* **19** 2320 (1997)
127. Hurd M *Phys. Rev. B* **55** R11993 (1997)
128. Abrikosov A A, Gor'kov L P *Zh. Eksp. Teor. Fiz.* **39** 1781 (1960) [*Sov. Phys. JETP* **12** 1243 (1961)]
129. Hirschfeld P J, Wölfle P, Einzel D *Phys. Rev. B* **37** 83 (1988)
130. Borkowski L S, Hirschfeld P J *Phys. Rev. B* **49** 15404 (1994)
131. Fehrenbacher R, Norman M R *Phys. Rev. B* **50** 3495 (1994)
132. Posazhennikova A I, Sadovskiĭ M V *Pis'ma Zh. Eksp. Teor. Fiz.* **63** 347 (1996) [*JETP Lett.* **63** 358 (1996)]
133. Posazhennikova A I, Sadovskiĭ M V *Zh. Eksp. Teor. Fiz.* **112** 2124 (1997) [*JETP* **85** 1162 (1997)]
134. Gor'kov L P, Kalugin P A *Pis'ma Zh. Eksp. Teor. Fiz.* **41** 208 (1985) [*JETP Lett.* **41** 253 (1985)]
135. Xiang T, Wheatley J M *Phys. Rev. B* **51** 11721 (1995)
136. Kampf A P, Devereaux T P *Phys. Rev. B* **56** 2360 (1997)
137. Riera J et al. *Phys. Rev. B* **54** 7441 (1996)
138. Poilblanc D, Scalapino D J, Hanke W *Phys. Rev. Lett.* **72** 884 (1994)
139. Hirschfeld P J, Goldenfeld N *Phys. Rev. B* **48** 4219 (1993)
140. Gor'kov L P *Zh. Eksp. Teor. Fiz.* **37** 1407 (1959) [*Sov. Phys. JETP* **10** 998 (1959)]
141. Carbotte I P et al. *Phys. Rev. B* **51** 11798(1995)
142. Basov D N et al. *Phys. Rev. B* **49** 12165 (1994)
143. Graf M J et al. *Phys. Rev. B* **51** 10588 (1995)
144. Hirschfeld P J, Putikka W O, Scalapino D J *Phys. Rev. B* **50** 10250 (1994)
145. Quinlan S M, Hirschfeld P J, Scalapino D J *Phys. Rev. B* **53** 8575 (1996)
146. Basov D N et al. *Phys. Rev. Lett.* **74** 598 (1995)
147. Anderson P W *Phys. Rev.* **109** 1492 (1958)
148. Maeckawa S, Fukuyama H *J. Phys. Soc. Jpn.* **51** 1380 (1981)
149. Ma M, Lee P A *Phys. Rev. B* **32** 5658 (1985)
150. Lee P A *Phys. Rev. Lett.* **71** 1887 (1993)
151. Balatsky A V, Salkola M I *Phys. Rev. Lett.* **76** 2386 (1996)
152. Balatsky A V, Salkola M I, Rosengren A *Phys. Rev. B* **51** 15547 (1995)
153. Franz M, Kallin C, Berlinsky A J *Phys. Rev. B* **54** R6897 (1996)
154. Balatsky A V, Rosengren A, Altshuler B L *Phys. Rev. Lett.* **73** 720 (1994)
155. Vails O T, Bëal-Monod M T *Phys. Rev. B* **51** 8438 (1995)
156. Bëal-Monod M T, Maki K *Phys. Rev. B* **53** 5775 (1996)
157. Haran G, Nagi A D S *Phys. Rev. B* **54** 15463 (1996)
158. Hirschfeld P J, Quinlan S M, Scalapino D J *Phys. Rev. B* **55** 12742 (1997)
159. Salkola M I, Balatsky A V, Schrieffer J R *Phys. Rev. B* **55** 12648 (1997)
160. Simon S H, Lee P A *Phys. Rev. Lett.* **78** 1548 (1997)
161. Haas S et al. *Phys. Rev. B* **56** 5108 (1997)
162. Enz C P *Phys. Rev. B* **54** 3589 (1996)
163. Bulut N, Scalapino D J *Phys. Rev. B* **54** 14971 (1996)
164. Mierzejewski M, Zielinski J *Phys. Rev. B* **56** 11925 (1997)
165. Zutic I, Vaels O T *Phys. Rev. B* **56** 11279 (1997)
166. Cassanello C R, Fradkin E *Phys. Rev. B* **56** 11246 (1997)
167. Ohta Y, Yamaguchi M, Eder R *Phys. Rev B* **56** 11262 (1997)
168. Dahm T, Manske D, Tewordt L *Phys. Rev. B* **56** R11419 (1997)
169. Makhlin Yu G *Phys. Rev. B* **56** 11872 (1997)
170. Han Q, Zhang L *Phys. Rev. B* **56** 11942 (1997)
171. Yang K, Sondhi S L *Phys. Rev. B* **57** 8566 (1998)
172. Martin A M, Annett J F *Phys. Rev. B* **57** 8709 (1998)
173. Wu W C, Carbotte J P *Phys. Rev. B* **57** R5614 (1998)
174. Willemin M et al. *Phys. Rev. B* **57** 6137 (1998)
175. Modre R, Schürrer I, Schachinger E *Phys. Rev. B* **57** 5496 (1998)
176. Riedel R A, Bagwell P F *Phys. Rev. B* **57** 6084 (1998)
177. Zhu J-X, Ting C S *Phys. Rev. B* **57** 3038 (1998)
178. Wang Z D, Wang Q-H *Phys. Rev. B* **57** R724 (1998)
179. Bang Y *Phys. Rev. B* **57** 142 (1998)
180. Yamada K et al. *Phys. Rev. B* **57** 6165 (1998)
181. Dai P, Mook H A, Dogan F *Phys. Rev. Lett.* **80** 1738 (1998)
182. Revaz B et al. *Phys. Rev. Lett.* **80** 3364 (1998)
183. Fleck M et al. *Phys. Rev. Lett.* **80** 2393 (1998)
184. Balatsky A V *Phys. Rev. Lett.* **80** 1972 (1998)
185. Gor'kov L P, Schrieffer J R *Phys. Rev. Lett.* **80** 3360 (1998)
186. Ioffe L B, Millis A J *Usp. Fiz. Nauk* **168** 672 (1998) [*Phys. Usp.* **41** 595 (1998)]
187. Schmalian J, Pines D, Stojkovic B *Phys. Rev. Lett.* **80** 3839 (1998)
188. Anderson P W *Adv. Phys.* **46** 3 (1997)
189. Anderson P W *J. Phys. Cond. Matt.* **8** 10083 (1996)
190. Anderson P W *The Theory of Superconductivity in the High-T_c Cuprates* (Princeton, N.J.: Princeton Univ. Press, 1997)
191. Mathur N D et al. *Nature* (London) **394** 39 (1998)